IEEE Access
Multidisciplinary ⋮ Rapid Review ⋮ Open Access Journal

Received 20 April 2024, accepted 24 June 2024, date of publication 28 June 2024, date of current version 8 July 2024.

Digital Object Identifier 10.1109/ACCESS.2024.3420693

TOPICAL REVIEW

Artificial Neural Networks for Photovoltaic Power Forecasting: A Review of Five Promising Models

RAFIQ ASGHAR[1], FRANCESCO RIGANTI FULGINEI[1], MICHELE QUERCIO[1], AND ASSIA MAHROUCH[2]

[1]Department of Industrial, Electronic and Mechanical Engineering, Roma Tre University, 00146 Rome, Italy

[2]Engineering for Smart and Sustainable Systems Research Center, Mohammed V University in Rabat, Rabat 10090, Morocco

Corresponding author: Rafiq Asghar (rafiq.asghar@uniroma3.it)

ABSTRACT Solar energy is largely dependent on weather conditions, resulting in unpredictable, fluctuating, and unstable photovoltaic (PV) power outputs. Thus, accurate PV power forecasts are increasingly crucial for managing and controlling integrated energy systems. Over the years, advanced artificial neural network (ANN) models have been proposed to increase the accuracy of PV power forecasts for various geographical regions. Hence, this paper provides a state-of-the-art review of the five most popular and advanced ANN models for PV power forecasting. These include multilayer perceptron (MLP), recurrent neural network (RNN), long short-term memory (LSTM), gated recurrent unit (GRU), and convolutional neural network (CNN). First, the internal structure and operation of these models are studied. It is then followed by a brief discussion of the main factors affecting their forecasting accuracy, including forecasting horizons, meteorological conditions, and evaluation metrics. Next, an in-depth and separate analysis of standalone and hybrid models is provided. It has been determined that bidirectional GRU and LSTM offer greater forecasting accuracy, whether used as a standalone model or in a hybrid configuration. Furthermore, hybrid and upgraded metaheuristic algorithms have demonstrated exceptional performance when applied to standalone and hybrid ANN models. Finally, this study discusses various limitations and shortcomings that may influence the practical implementation of PV power forecasting.

INDEX TERMS Artificial neural network, solar energy, PV power, forecasting horizons, performance analysis, limitations.

I. INTRODUCTION

A. BACKGROUND

Modern economies depend on reliable energy sources to supply electricity for every facet of human life, from agribusiness and healthcare to industry and education to environmental preservation [1], [2]. Fossil fuels remain a dominant energy source globally, accounting for 83.1% of global energy production in 2020 [3]. However, using fossil fuels for energy has several negative impacts on humans and the environment. They emit significant amounts of greenhouse gases into the atmosphere, leading to air and water pollution. In addition, their resources are dwindling at an alarming pace [4]. In recent decades, solar energy has emerged as a popular option for energy shortages and a viable alternative to fossil fuels. This energy source, which is both renewable and environmentally friendly, provides an inexhaustible and sustainable source of electricity. In 2022, PV power output reached approximately 1,062 GW, as shown in Fig. 1 [5], and for the first time, it surpassed wind power production [5], [6]. The international energy agency (IEA) projects that solar energy will surpass natural gas and coal by 2026 and 2027, assuming yearly capacity additions continue to rise at the same pace over the following five years. By 2030, the annual increase in PV power capacity will reach 630 GW, four times higher than the record levels attained in 2020 [7]. In 2050, there will be 14,000 GW of accumulated PV capacity, and solar energy will provide approximately half of the world's energy demand [8]. Thus, solar energy has the potential to meet the world's energy needs. However, it primarily depends

The associate editor coordinating the review of this manuscript and approving it for publication was Sudhakar Babu Thanikanti.

on weather conditions, and any fluctuations in weather conditions may significantly impact its output power [9], [10], [11]. Variations in PV power output can cause system instability, mainly when PV power accounts for a significant portion of the energy supply. Accurate forecasting is critical for effectively integrating PV power into electrical grids and mitigating the negative impacts of variable PV power output on the system. Thus, various research has been published during the last decade, proposing innovative and promising

models for PV power forecasting across different geographical regions and periods. These models include physical, statistical, artificial intelligence (AI), and hybrid models [10], [13]. Physical models use numerical weather forecasts and satellite observations to predict solar radiation [14]. Given the availability of appropriate input data, these models can provide accurate predictions. However, they may give unsatisfactory results when attempting to include complex dynamics and variations in the data. Statistical models use historical data to identify patterns and correlations between input variables, such as meteorological conditions and PV power output [15]. Although these models may be helpful in specific situations, they have several limitations, including their simplicity, sensitivity to outliers, and dependence on historical data. Thus, novel modelling tools, such as AI and hybrid models, are necessary to assess the nonlinear interactions between input factors and PV power forecasting. Studies have shown that AI models outperform conventional physical and statistical models when forecasting PV power [16]. These models may learn from past data and form strong associations between important features. Nevertheless, conventional AI models like support vector machines (SVM), random forests (RF), and decision trees (DT) possess a shallow framework and limited learning capacity. In addition, these models have limited generalization capacity. ANN is a robust and intelligent AI tool for modelling, forecasting, and optimizing the performance of diverse engineering systems. This approach has successfully addressed complex nonlinear engineering problems () [17], [18], [19]. These features become critical when dealing with the dynamic nature of environmental conditions. Hence, ANNs have become increasingly prominent in the solar energy sector, particularly for fault detection, predictive maintenance, radiation forecasting, and power prediction applications.

B. LITERATURE REVIEW

Various ANN-based models have been developed in the literature, including RNN, CNN, radial basis function neural network (RBFNN), and hybrid models with different characteristics and benefits. These models are evaluated and validated using various metrics, including mean absolute error (MAE), root mean square error (RMSE), mean absolute percentage error (MAPE), relative root mean square error (RRMSE), correlation coefficient (R), and normalized mean bias error (NMBE). Over the last few decades, researchers have focused on improving neural network topologies, optimizing training procedures, and enhancing the accessibility of high-quality data. Thus, modern ANNs are particularly adept at identifying complex geographical and temporal patterns within solar irradiance data, ultimately improving predictions' accuracy. A study found that when predicting solar radiation, an RNN model performed better than a conventional ANN model in terms of NMBE (47%) and RMSE (26%) [20]. The RNN model is capable of capturing the temporal variations in PV output, resulting in more accurate forecasting errors compared to traditional methods like multiple linear regression (MLR) and bagged regression trees (BRT) [21], [22]. CNN, another type of ANN, has recently received much attention due to its remarkable performance in image classification, speech recognition, and object detection [23]. For PV power forecasting, CNN can provide accurate prediction results that are more stable over a range of sequence lengths than conventional ANN [24]. In comparison to MLR and ANN, which achieve MAPEs of 16.187% and 15.991%, respectively, a multi-channel CNN achieves a MAPE of 8.639% for predicting monthly PV power [25]. To further enhance CNN's performance, a hybrid GA/PSO technique is implemented to optimize the relevant hyperparameter [26]. The proposed approach reduces the MAE by an average of 0.1463 MJ.m^{-2} compared to a single CNN architecture. Aside from various ANN models, some research developed integrated or hybrid models to improve forecasting accuracy. A hybrid model integrating CNN and LSTM is proposed for predicting PV power production, and the results are compared to those of CNN and LSTM models [27]. In terms of accuracy, the hybrid model outperforms the single model by 54.92%, 49.10%, and 31.37%, respectively, when compared to the LSTM model and 4.70%, 14.29%, and 14.63% when compared to the CNN model. Similarly, the CNN-LSTM hybrid model is optimized using a sine-cosine algorithm (SCA), which the authors claim performs better than the CNN-LSTM hybrid model without the SCA [28].

C. MOTIVATION AND CONTRIBUTIONS

With the growing integration of PV power, forecasting has become more critical. More advanced modelling approaches have been applied in recent years, resulting in better forecasting accuracy. Some studies have presented in-depth analyses of these approaches to identify potential gaps for future research [10], [29], [30], [31], [32], [33], [34]. These publications used conventional ANN models for the analysis or included modelling approaches that would be useful up to 2020. In addition, these studies did not provide a comprehensive overview of recent advances in ANN models such as LSTM, GRU, CNN, BiLSTM, and BiGRU. These studies also lack the separate analysis and comparison of the standalone and hybrid models necessary to provide the reader with a clear picture. Hence, a comprehensive assessment of PV power forecasting using advanced ANN models is required. This research systematically reviews the most recent developments in PV power forecasting, focusing on

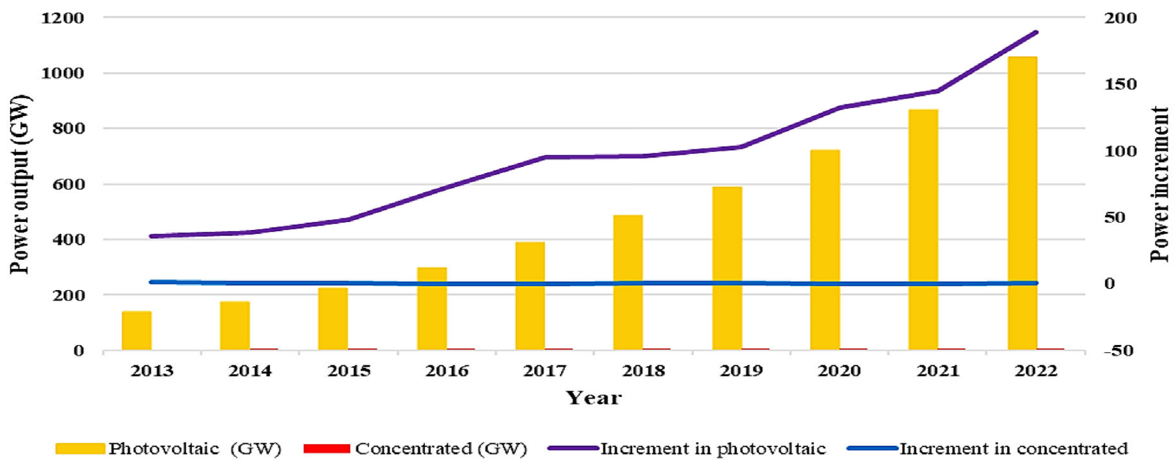

FIGURE 1. PV power generation for the recent decade, from 2013 to 2022 [12].

five widely used ANN models. Multiple parameters have been adopted to evaluate the performance of these models. The important contributions of this study are outlined below:

- An in-depth overview of the different types of ANNs, such as MLP, RNN, LSTM, GRU, and CNN, is presented.
- Both standalone and hybrid models for PV power forecasting are briefly studied and compared.
- Multiple factors, including forecasting horizons, meteorological conditions, evaluation metrics, and others that impact forecasting accuracy, are also thoroughly explained.
- Various limitations and shortcomings related to applying ANN models for PV power forecasting are also explored.
- Finally, findings and recommendations for further study are provided.

The rest of the paper is arranged as follows. Section II presents a detailed history of ANN and examines the design and operation of five ANN models. Section III explores multiple factors, including forecasting horizons, meteorological conditions, and evaluation measures affecting PV power forecasts. Section IV reviews the application of standalone and hybrid models for PV power forecasting. Section V summarizes the findings of both standalone and hybrid models, while Section VI presents the potential limits of ANN models for PV power forecasting. Section VII concludes the work and offers future research directions.

II. ARTIFICIAL NEURAL NETWORKS

A. HISTORY OF NEURAL NETWORKS

The concept of ANNs has been shaped by the contributions of numerous scholars throughout its history. In 1943, Warren McCulloch and Walter Pitts developed a mathematical model of an artificial neuron [35], which is considered one of the earliest steps in the development of neural networks. In the 1950s, Rosenblatt introduced the perceptron, an ANN consisting of a single layer of interconnected neurons that can learn binary categorization tasks [36]. However, perceptrons require real-time computations, which digital computers could not perform efficiently in the 1950s. In 1960, Hoff and Widrow developed the adaptive linear neuron (ADALINE) model [37]. It was a single-layer neural network trained using the delta rule to reduce the MSE between observed and target values. Like a perceptron, this model was developed for binary classification; thus, its capacity to model complex relationships was limited. Minsky and Papert considered extending single-layer perceptrons to multiple layers, feeding each layer into the next layer [38]. However, concerns were raised about the feasibility of training these advanced multilayer perceptrons. Thus, many participants considered this confusion decisive, leading to abandoning the field. In 1982, Hopfield introduced a discrete neural network that advanced the field of neural networks significantly. For the first time, this seminal work introduced the concept of the Lyapunov function in neural network research [39]. In 1984, Hinton and Sejnowski introduced the Boltzmann machine [40], [41], a system of interconnected units that resemble neurons and can make probabilistic decisions regarding their activation state. Boltzmann machines possess a simple learning algorithm to identify intriguing features that capture complex patterns within the training data. In 1986, Rumelhart and Hinton revived the backpropagation (BP) algorithm, which has been experimentally shown to be capable of learning complex tasks on multilayer networks [42], [43]. It was a significant development that stimulated renewed interest in neural networks. In 1997, Hochreiter and Schmidhuber developed the LSTM, which was designed to overcome the vanishing gradient problem encountered by RNNs [44]. LeNet, the first CNN architecture, was designed by LeCun et al. for handwritten digit recognition issues in 1998. LeNet struggled to train because of the vanishing gradients problem, but max-pooling across convolutional layers is used to reduce image size, thereby preventing overfitting and enhancing CNN training

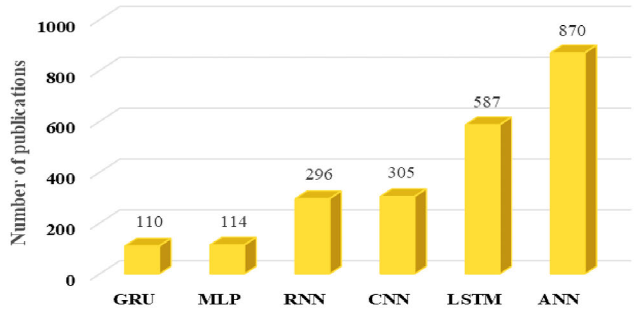

FIGURE 2. Number of articles on ANN relating to PV power forecasting.

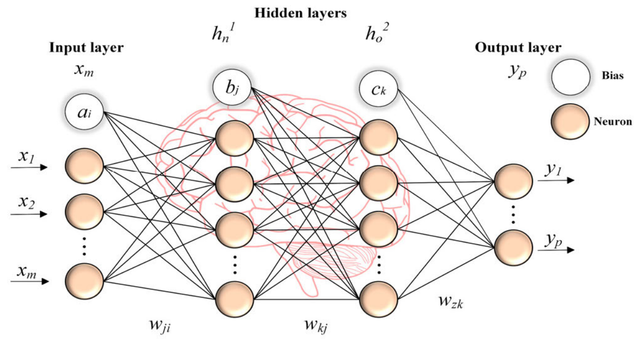

FIGURE 3. Multilayer perceptron architecture.

[45]. In 2005, Graves et al. presented bidirectional-LSTM (BiLSTM), an algorithm that is ideally adapted for time series problems and can be applied to both forward and backward information [46]. In 2014, Cho et al. proposed the gated recurrent unit (GRU), a type of RNN model with a simpler design that addresses the same problems as LSTM [47]. In 2015, Kaiming et al. introduced the residual neural network (ResNet), which employs residual connections to address the vanishing gradient problem, a common issue in training deep neural networks [48].

B. TYPES OF NEURAL NETWORKS

Over time, different types of ANNs have been designed to address specific problems, applications, and data sets. These include MLP, RNN, CNN, and hybrid neural networks. Furthermore, two types of RNNs, LSTM and GRU, are also widely researched due to their exceptional performance when applied to time series data. Fig.2 shows the five most commonly used models for PV power forecasting based on data from the Scopus database from 2017 to 2023. Hence, this section will study these five ANN models' internal structure, design, and operation.

1) MULTILAYER PERCEPTRON

MLP is the most fundamental and effective data-driven modelling tool in ANNs [49]. An MLP having one input layer, two hidden layers, and one output layer can be depicted in Fig.3 [50]. The input layer is the initial step of data input in the MLP. This layer collects the input variables from the outside environment, such as solar radiation, ambient temperature, wind speed, humidity, clearness, dust, and cloud cover from the outer environment [51]. These variables allow the MLP to comprehend and learn the complex relationships between environmental parameters and PV power generation. Hence, it is essential to preprocess and organize these input variables before feeding them to the MLP. The input variables are then passed to the hidden layer, located between the input and output layers. The hidden layers are essential for optimal MLP performance, mainly when accuracy and time complexity are the primary concerns [52]. Neurons in the hidden layers receive the input value from the input layer and calculate the weighted sum of that value. Then, each neuron applies an activation function such as the sigmoid, softmax, rectified linear unit (ReLU), parametric ReLU, swish, or gaussian error linear unit (GELU) to the weighted sum. An activation function determines whether a neuron should be activated based on its input's significance. Moreover, the activation function incorporates nonlinearity into the model, allowing the MLP to recognize and learn complex data patterns. All neurons' activation outputs are combined to produce an output, which is transmitted to the model's output layer; this output represents the MLP's prediction for PV power output. Consider a four-layer MLP model (one input, two hidden, and one output) as depicted in Fig. 3. There are m input variables in the input node ($x_i, i = 1, 2, 3, \ldots, m$) and p output variables in the output node ($y_l, l = 1, 2, 3, \ldots, p$). The network consists of two hidden layers with n number of nodes in layer 1 and o number of nodes in layer 2 (such that $h_j, j = 1, 2, 3, \ldots, n$ and $h_k, k = 1, 2, 3, \ldots, o$). Equations (1), (2), and (3) provide a mathematical description of the MLP model:

$$h_m = f_h\left(\sum\nolimits_{i=1}^{m} x_i w_{ji} + a_i\right) \tag{1}$$

$$h_o = f_h\left(\sum\nolimits_{j=1}^{o} h_j w_{kj} + b_j\right) \tag{2}$$

$$y_p = f_y\left(\sum\nolimits_{k=1}^{p} h_k w_{lk} + c_k\right) \tag{3}$$

w_{ji}, w_{ji}, and w_{ji} represent the weight parameters, a_i, b_j, and c_k represent the bias, and f_h and f_y represent the activation functions.

2) CONVOLUTIONAL NEURAL NETWORK

A CNN is a feedforward deep neural network first inspired by Hubel and Wiesel [53]. CNNs are designed to replicate living beings' visual perception mechanisms and can perform supervised and unsupervised learning. CNNs' greatest strength is its ability to reduce the number of parameters, encouraging researchers to handle more complex models previously unsolvable for traditional ANNs [54]. Consequently, CNN has produced ground-breaking results in various domains, including medical imaging, computer vision, art creation, natural language processing, voice recognition, defect detection, pattern recognition, forecasting, and environmental monitoring. As depicted in Fig. 4, CNN consists of multiple

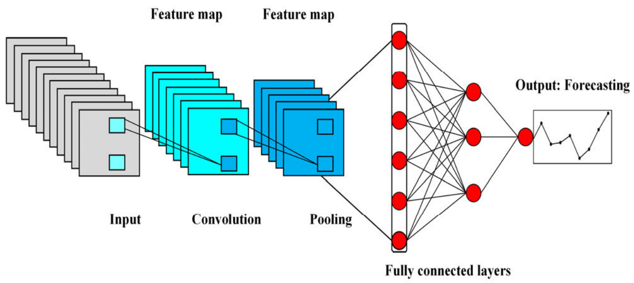

FIGURE 4. Typical CNN architecture.

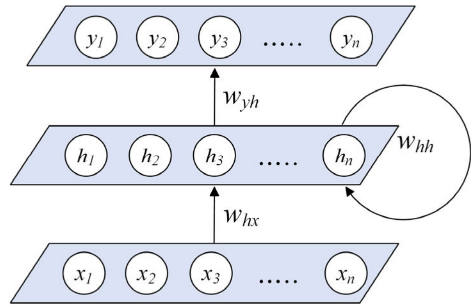

FIGURE 5. A folded architecture of RNN.

layers: convolution, pooling, fully connected, and output. Convolutional layers are vital in designing CNNs since they facilitate extracting localized features from the input data [55]. These layers apply convolution to the preceding layer's feature maps, followed by a non-linear activation function such as ReLU. This non-linear activation introduces non-linearity into the network more accurately to reflect complex non-linear relationships in the data. The operation of the convolutional layer can be illustrated as follows [56].

$$x_s^n = f\left(\sum\nolimits_{r\in M_s} x_r^{n-1} * k_{rs}^n + b_s^n\right) \tag{4}$$

where x_s^n denotes the sth output feature map, f the activation function, n the number of layers, k the convolution kernel, and b the bias. After the convolutional layer, the pooling layer executes a down-sampling process that helps reduce the feature maps' dimensions [57]. Its key goals are (1) reducing the number of parameters and, thus, the computing cost and (2) avoiding overfitting. Implementing the pooling layer is expected to compute a feature map's average or maximum pooling value [55], [58].

$$x_r^n = f\left(B_r^n * dow\left(x_r^{n-1}\right) + b_r^n\right) \tag{5}$$

where dow represents the pooling function, x_r^{n-1} represents the feature map of the $n-1$th layer, and B_r^n represents the bias. After a series of convolution and pooling layers, all inputs are sent to a fully connected layer, determining the final output [59].

$$y^n = f\left(w^n * y^{n-1} + b^n\right) \tag{6}$$

where y^n represents the final output vector, w^n represents the weight, and b^n represents the bias.

3) RECURRENT NEURAL NETWORK

RNNs are a subtype of ANN explicitly designed to model sequential or time-series data for the recognition and prediction of sequences [55]. Time-series data incorporates inherent temporal information that a conventional neural network cannot capture. RNNs are designed with a form of memory that enables them to maintain a hidden state capable of storing data from previous time steps in a sequence. A high-dimensional hidden state and nonlinear development give the RNN's hidden state tremendous expressive capability, allowing it to integrate information over multiple timesteps and provide precise predictions [60]. However, traditional RNNs have a limited memory capacity, which limits their ability to simulate long-range structures. Due to their inability to form stable memories, their capacity to generate sequences is unstable [61]. In such cases, it is common for predictions to deviate from the manifold on which the training data is located.

Consider a conventional RNN as depicted in Fig. 5 that receives an input vector sequence $(x_1, \ldots, x_n)$. The RNN calculates the hidden states (h_n) and outputs (y_n) by iteration of the corresponding equations [62].

$$h_n = f_h\left(x_n w_{hx} + h_{n-1} w_{hh} + b_h\right) \tag{7}$$
$$y_n = f_y\left(h_n w_{yh} + b_y\right) \tag{8}$$

where f_h and f_y represent activation functions, b_h and b_y represent bases, and w represents the weight matrix between the corresponding layers.

4) LONG SHORT-TERM MEMORY NEURAL NETWORK

LSTM networks are a refinement and expansion of RNNs that have shown great success in time series prediction problems [55], [63]. Due to gradient vanishing and gradient explosion problems, RNNs are ineffective when dealing with long-term data dependencies. Hochreiter et al. proposed the LSTM model to address these limitations, which can learn long-term dependencies in data [44], [55]. Thanks to their memory cells, these models can analyze and identify temporal patterns in data sequences. Due to the presence of memory cells, these models can generate accurate forecasts, and they have recently gained widespread use in predicting stock prices, weather, and energy consumption. However, compared to a standard RNN, LSTMs have around four times as many parameters, resulting in excessive complexity in the hidden layer [64]. Fig. 6 depicts the basic structure of an LSTM and the data transfer within an LSTM network. A standard LSTM unit is made up of many essential elements, including memory cells, an input gate (i_t), an output gate (o_t), and a forget gate (f_t). The cell can retain values for an arbitrary period, and its three gates control the influx and outflow of data. The cell state serves as a memory unit and is transmitted linearly through the LSTM chain, with minimum linear interactions [65], [66]. As depicted in the figure, the forget gate receives the output of the previous LSTM unit (h_{t-1}) and the current input (x_t). The sigmoid function (σ) determines which information is selected and which is disregarded. It examines the values of (h_{t-1}) and (x_t) and generates a 0 to 1 output for each cell state (C_{t-1}) element.

$$f_t = \sigma_f \left(w_f . [h_{t-1}, x_t] + b \right) \tag{9}$$

where w_f and b are the weight matrix and bias of the forget gate. In the subsequent stage, the input gate employs a sigmoid function (σ) to determine the values to be written and a hyperbolic tangent function ($tanh$) to create a new cell value (N_t) as seen in the following equation [65].

$$i_t = \sigma_i \left(w_i . [h_{t-1}, x_t] + b \right) \tag{10}$$

$$N_t = tanh \left(w_c . [h_{t-1}, x_t] + b \right) \tag{11}$$

Then, the previous state (C_{t-1}) is multiplied by the (f_t) and added to the product of i_t and N_t to update the new cell state (C_t).

$$C_t = C_{t-1} * f_t + N_t * i_t \tag{12}$$

Finally, the output gate (O_t) determined the amount of data to be transmitted to calculate the output (h_t) at the subsequent timestamp.

$$O_t = \sigma \left(w_o [h_{t-1}, X_t] + b \right) \tag{13}$$

$$h_t = O_t * tanh \left(C_t \right) \tag{14}$$

where w_c and w_o are the weight matrices and b is the bias

5) GATED RECURRENT UNIT NEURAL NETWORK

A GRU is another type of RNN proposed in 2014 [67] that performs the same function as an LSTM to overcome long-term dependency issues. This feature is beneficial for time-series data as it lowers the computational burden. Like an LSTM, a GRU comprises gating units that regulate the flow of information; however, it does not have separate memory cells [47]. The gate structures of a GRU are simpler than those of an LSTM, as shown in Fig. 6. The update gate in a GRU combines the functions of both the forget gate and input gate in an LSTM. The update gate decides which information from the previous state should be moved to the current state, whereas the reset gate decides whether new information will be added to the prior state. GRUs can maintain long-term dependencies in sequences, similar to LSTMs [68]. However, since they have fewer parameters and a faster training rate, GRUs are computationally more efficient. Another advantage of GRU is that its simple structure makes it less prone to overfitting. The reset gate (r_t) and update gate (u_t) of GRUs are defined by the following equations,

$$r_t = \sigma (w_r \cdot [h_{t-1}, x_t] + b) \tag{15}$$

$$u_t = \sigma \left(w_u \cdot [h_{t-1}, x_t] + b \right) \tag{16}$$

where w_r and w_u are the weights of the reset and update gates, respectively. After the computation of the reset gate, a candidate hidden state ($\acute{h_t}$) is determined using the ($tanh$). The candidate hidden state is formed by integrating the current input, the previous hidden state, and the reset gate in the following manner:

$$\acute{h_t} = tanh \left(w_{\acute{h}} \cdot [h_{t-1}, x_t] + b \right) \tag{17}$$

The final hidden state (h_t) is then determined using linear interpolation, which incorporates both the past and future hidden states and is influenced by the update gate in terms of degree.

$$h_t = (1 - u_t) * h_{t-1} + u_t * \acute{h_t} \tag{18}$$

where $w_{\acute{h}}$ is the weight of the candidate's hidden state.

III. PHOTOVOLTAIC POWER FORECASTING

The erratic nature of PV power can significantly impact the power grids' operation. PV power can fluctuate from maximum to minimum in seconds, impacting the operation of other interconnected systems. This impact becomes more significant when a considerable amount of PV power is integrated into the electrical system [69]. The fluctuation of PV power in a connected electrical system may lead to voltage changes, power outages, infrastructure damage, and even catastrophic failures [70]. Accurate PV power forecasts would reduce these challenges and provide more reliable and economical methods for meeting the minimum generation and scaling requirements. Accurate forecasting can motivate plant managers to generate more accurate bids and schedule maintenance downtime more efficiently [31]. Multiple factors, including the forecasting timeframe, meteorological conditions, evaluation metrics, and others, contribute to the inaccuracy of PV power forecasting. In some power markets, inaccuracies may result in penalties if the difference between the forecast and actual power production exceeds a specific tolerance range. For instance, the authors estimated the cost of forecasting errors for a solar thermal power plant in Spain [71]. Forecasting error is divided into groups ranging from 10% to 100%. According to the findings, penalties per MWh increase from 10-20% to 60-70% for relative prediction errors while remaining relatively constant at about 6 €/MWh for larger forecast errors. An overestimated PV power would require a different set of generators to respond than initially planned [72]. In contrast, underestimating PV power output can lead to transmission congestion, and curtailment, and require an adjustment to the scheduled generator configuration. A thorough analysis of various factors affecting PV power forecasts is presented in this section.

A. FORECASTING HORIZONS

Accurate forecasting has been a major focus in integrating PV power into the electrical grid. These forecasts often use ANNs, which access a wide range of data sources to forecast power variations with a lead time of minutes or hours. Depending on the forecasting horizon, PV power predictions range from seconds to years ahead. Generally, the

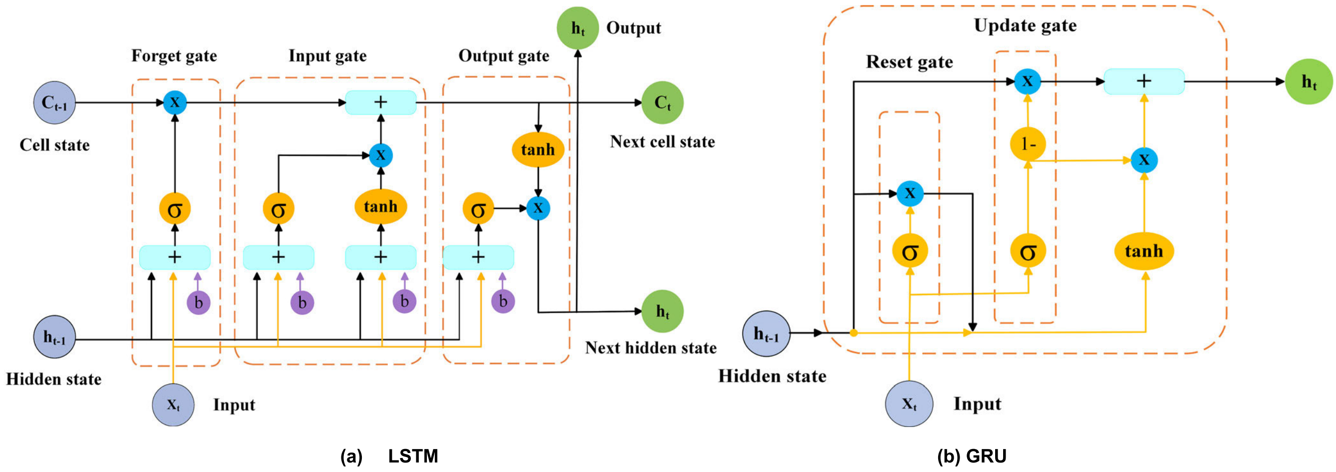

FIGURE 6. The architecture and flow of data in LSTM and GRU [68], [73], [74].

forecasting horizon is categorized into three periods: short-term, medium-term, and long-term. The literature introduces a fourth category, very short-term forecasting, which the researcher claims to be effective in facilitating real-time optimizations [55]. Fig. 7 depicts four forecasting horizons outlined in the literature and their application to PV power production [75]. The forecasting horizon is an important factor that influences the accuracy of PV power prediction.

1) VERY SHORT-TERM FORECASTING

Very short-term forecasting predicts PV power production a few minutes to one hour in advance [76]. Some studies have considered this timescale ranging from a few seconds to 30 minutes [77], while others have considered 5 to 60 minutes in advance [78], [79]. Grid operators use these forecasts to plan output power, control load frequency, manage demand response, and maximize reserve energy sources [80]. These forecasts can also be used for energy marketing, pricing, power stability, monitoring real-time power dispatch, and managing PV storage. Very short-term is important for controlling the unpredictable and rapidly changing behaviour of PV power production. PV power production can fluctuate by over 50% in less than one minute [81]. Studies show that the PV power output can change from maximum to minimum within one second [82]. Such large fluctuations can cause significant issues for power systems, including power mismatch, voltage fluctuations, and frequency instability [83]. In the past, these forecasts were not given as much emphasis; however, with the growing significance of real-time forecasting and increased PV power worldwide, the significance of very short-term forecasting has also increased. Since very short-term forecasts need real-time data, they are more difficult to estimate than other forecasting horizons.

2) SHORT-TERM FORECASTING

Short-term forecasting normally ranges from one hour to one day in advance. Some researchers describe the short-term forecasting horizon as spanning a few hours or even seven days [10]. Short-term forecasting is highly applicable in power market control. These forecasts assist in optimal generation scheduling, load dispatch choices, large energy storage, and balancing supply and demand [55]. These forecasts may also ascertain the optimal PV power ramp rate. Thus, they enhance the power grid's security and facilitate the development of an integrated PV energy management system [84]. Short-term forecasting may help asset owners and market participants make more informed bids in energy markets. As a result, using accurate forecasting while putting bids would reduce the probability of incurring penalties for imbalances [85]. Over the last three years, there has been a significant increase in studies on short-term forecasting, aligning with the worldwide expansion of PV power generation. Hence, these forecasting techniques for solar PV power generation are becoming more critical as their integration into the power grid expands.

3) MEDIUM-TERM FORECASTING

Medium-term forecasting predicts PV power generation for one to several days in advance. Some studies have defined the forecasting horizon as 6 to 24 hours [86], while others concentrated on a timescale ranging from one week to one month in advance [10]. These forecasts are important for determining the maintenance schedule of solar power plants, which include transformers and other equipment, to minimize losses. In addition, medium-term forecasting is crucial for asset optimization, generating unit control, unit scheduling, power system planning, and risk management [87]. Despite their relevance in PV power and power system operation, medium-term forecasting models have received little attention, and there are few explanations for these forecasts in the literature.

4) LONG-TERM FORECASTING

Long-term forecasting includes a time horizon of several weeks to a year ahead [85]. Some researchers describe the range of forecasting horizons as one to ten years ahead [84].

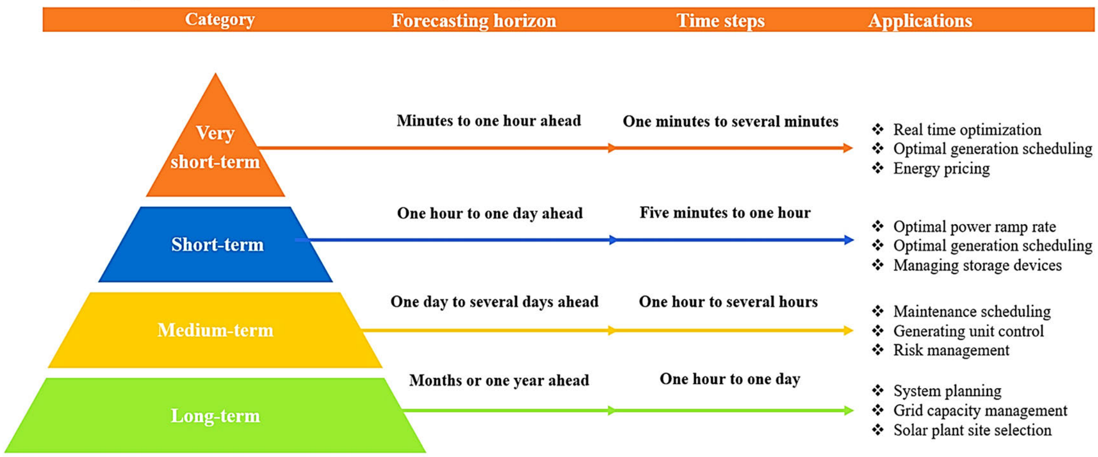

FIGURE 7. Classification and applications of forecasting horizons [75].

Long-term forecasts help develop long-term strategic plans that ensure the optimal operation of solar power systems [55]. System operators use these forecasts to manage better the grid's transmission, operating, and distribution capacity. In addition, these forecasts may help determine the best location, size, and configuration of PV arrays and energy storage devices for a solar power plant. Nevertheless, long-term forecasting is susceptible to a greater level of uncertainty in comparison to shorter-term forecasts [10]. This is due to a higher probability of various fluctuations in atmospheric conditions, which can introduce uncertainty into the systems. Climate patterns and other environmental elements include temporal changes that may affect weather systems and limit the accuracy of long-term forecasts.

B. WEATHER CONDITIONS

The ideal weather conditions for PV power generation are cold, sunny, and windy [88]. The solar panel harnesses solar energy, while the surrounding cold air and the cooling effect of the wind prevent any overheating caused by the device. However, the erratic and continuously changing weather conditions provide substantial challenges for accurate PV power production and forecasting models [89]. One study estimates that weather-related variables influence over 60% of PV power forecasts [90]. This significant weighting underscores the crucial influence of weather-related factors on the efficiency of photovoltaic systems. Weather-related variables influencing forecasting model accuracy include solar irradiance, cloud formation, wind speed, humidity, temperature, and aerosol concentrations [91]. However, in order of importance, these variables are solar radiation, sunshine, wind speed, temperature, cloud cover, and humidity [92]. The correlations between these variables and PV power production may be found using the Boruta algorithm [93]. Among these variables, solar irradiance and temperature are positively correlated, with corresponding Pearson correlation coefficient (r) of 0.88 and 0.5 [94]. The correlation coefficient of humidity, cloud cover, and precipitation is negative, as shown in Fig. 8. Regarding the correlation coefficient of wind speed, some authors consider it weakly positive. In contrast, others deem it to be a weekly negative [95]. The blue line shows the value of r between PV power generation and weather-related variables. In other words, an incremental rise of one standard deviation in sunshine led to a proportional surge of 4.7% in PV power production. Cloud cover adversely affects the output of PV arrays, leading to a decrease of 5.9%, while precipitation causes a 4.6% decline [96]. A direct correlation exists between the sun's elevation angle and forecasting accuracy [97]. This is because sunlight must travel a larger distance through the Earth's atmosphere, resulting in higher atmospheric absorption and dispersion. Consequently, the available solar energy drops, lowering the accuracy of PV power forecasts. Another issue is that researchers are training their forecasting models with weather-forecasted data. These models may provide unsatisfactory forecasts if they use uncorrelated weather data or weather variables with considerable errors [95]. The impact of these errors will become greater as the forecasting lead time is expanded. A case study examines observed and 6-day forecasted weather data for important parameters impacting power forecasting for the same setup of solar panels [95]. The MAPE error for the observed weather data is 13.47, which increases with each forecasted day's data until it reaches a maximum of 17.4 on day 5. Another study determined that forecasting errors in radiation, temperature, and wind speed resulted in over-estimating greenhouse power consumption [98]. However, radiation forecasting error has the highest influence among these three weather-related variables, with a mean relative error (MRE) of 6.1%. In general, weather forecasting errors are caused by shortcomings in the model itself and imprecise initial conditions [99]. Weather models are assumed to be stochastic and vulnerable to modest changes in initial conditions; much emphasis has been placed on the latter as a barrier to forecasting. Hence, accurate weather forecasting is vital owing to the adverse effects of these variables on PV power forecasts. This is particularly important given the increased weather fluctuations and rapid proliferation of PV technology.

C. EVALUATION METRICS

An evaluation metric is an analytical and mathematical method that determines how closely projected and actual outputs coincide [100]. Evaluation metric, also known as performance metric or error metric, is an essential component for analyzing the performance of forecasting models. These metrics prove why forecasting models are useful and practical in providing a high level of competence in addressing difficult and complex issues across multiple domains [101]. They are also crucial in the model's optimization and fine-tuning since they indicate the best values for model hyperparameters and network choices. Various evaluation metrics are used depending on the specific task and purposes of the network. Table 1 summarizes different evaluation metrics for regression and classification models. In the regression model, evaluation metrics compare the model's predictions to the actual values of the data set [102]. The greater the difference between actual and predicted values, the less accurate the model is. The difference can be caused by various factors, including the model's complexity, data quality and quantity, and the algorithm's suitability. In regression models, evaluation metrics are further divided into four distinct categories: primary, extended, composite, and hybrid [100], [103]. This categorization helps data scientists and researchers identify the best metrics for assessing regression models depending on their goals, data type, and model domain. In the case of classification models, the primary purpose of evaluation metrics is to assess the model's success in allocating instances to various groups or categories. These models use evaluation metrics to evaluate the classifier's performance [104]. Classification metrics are categorized into threshold, probability, and ranking [104], [105]. In threshold classification, the main objective is to allocate instances or data points to one of several specified groups or categories. The probability classification method classifies instances by their associated probabilities, whereas the ranking classification method classifies instances by importance. Classification model metrics are typically implemented in two phases: training and testing. During training, these metrics are used to fine-tune the classification algorithm, whereas during testing, they are used to evaluate the classifier's performance with data it has never seen.

IV. APPLICATION OF ANN FOR PHOTOVOLTAIC POWER FORECASTING

Accurate PV power forecasting continues to be a considerable challenge, owing to various contributing factors [84]. Weather conditions, geographical factors, forecasting horizons, and technical aspects contribute to forecasting complexity. Standard forecasting models often struggle to learn the complex and non-linear correlations among these factors, resulting in reduced forecasting accuracy. Addressing these problems needs a comprehensive strategy, including advances in modelling approaches, increased data quality, and deep knowledge of the complex dynamics of PV power forecasting [106]. ANNs may forecast solar power production by identifying complex patterns from massive datasets and capturing the complex relationships between power output and influencing factors [84]. Compared to other machine learning (ML) models, these models may give better accuracy for PV power prediction. For instance, the authors compared an ANN model to five different ML models: RF, DT, support vector regression (SVR), generalized additive model (GAM), and extreme gradient boosting (XGBOOST) [107]. The purpose of this comparison was to forecast energy output from a 24 kWc solar facility in Morocco. The results indicate that the ANN model outperformed the other five models, exhibiting better values for all evaluation measures, as shown in Fig. 9. For PV power forecasting, four ML models—ANN, SVM, K-nearest neighbors (KNN), and linear regression (LR)—are reviewed for a 13 kWp solar power plant in Medellin, Colombia [108]. The ANN model gives the lowest RMSE (86.466 W) and MAE (8.409 W) errors, whereas the LR method and SVM produce the maximum RMSE (94.583 W) and MAE (9.6209 W), respectively. Similarly, ANN, SVM, and regression models are considered for day-ahead PV power forecasting using meteorological parameters [109]. ANN outperforms SVM and regression models and provides superior results for RMSE (468.2), MAE (186.8), MAPE (6.538), and R^2 (0.838). Several upgraded versions of ANN have been presented in the literature, displaying greater accuracy and convergence rate than standard ANN. Researchers have also employed hybrid strategies, such as merging predictions from several standalone ANN models or mixing ANN models with other ML models or statistical models (autoregressive integrated moving average (ARIMA), seasonal-ARIMA). Hybrid models outperform standalone alternatives in accuracy, resilience, and flexibility. However, the choice of a model depends upon a multitude of factors, encompassing computational resources, data requirements, interpretability, explainability, and transparency.

A. STANDALONE MODELS

ANNs are widely used in PV power forecasting problems due to their flexible structure [110]. Their data-driven techniques greatly improve the extraction and analysis of critical information from large datasets [111], [112]. Over time, advanced ANN models are proposed to increase the accuracy of PV power forecasts for various geographical regions, as shown in Table 2. MLPs are highly recognized for their ability to handle large datasets effectively. These models can precisely approximate any nonlinear function and are often used in regression problems where the aim is to estimate an output variable using predictor variables [113], [114]. Several studies have demonstrated that MLPs can be used to provide

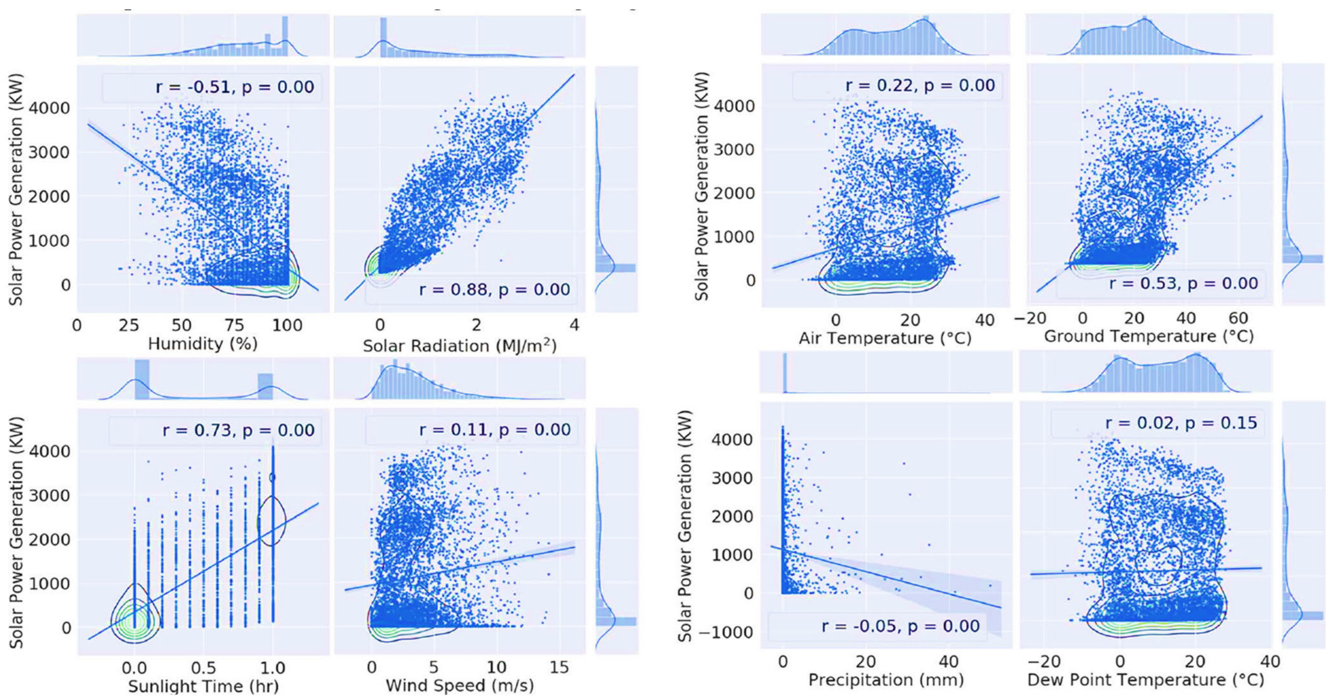

FIGURE 8. Correlation between PV power generations and weather-related variables [94].

TABLE 1. Summary of various evaluation metrics.

Application	Metrics	Descriptions	Formula
Regression models	MAE	Measures the average magnitude differences between actual and predicted values.	$\frac{1}{n}\sum_{i=1}^{n}\lvert p_{a,i}-p_{f,i}\rvert$
	MSE	Measures the average squared difference between actual and predicted values.	$\frac{1}{n}\sum_{i=1}^{n}(p_{a,i}-p_{p,i})^2$
	MRE	The ratio between the mean absolute error (MAE) and the actual value.	$\frac{1}{n}\sum_{i=1}^{n}\frac{(a_i-p_i)}{a_i}$
	RMSE	Measures the square root of the average squared difference between actual and predicted values.	$\sqrt{\frac{1}{n}\sum_{i=1}^{n}(p_{a,i}-p_{p,i})^2}$
	MAPE	Measures the average percentage difference between actual and predicted values.	$\frac{1}{n}\sum_{i=1}^{n}\frac{\lvert p_{a,i}-p_{p,i}\rvert}{a_i}\times 100\%$
	NMBE	Measures the relative mean bias between the actual and predicted values.	$\frac{1}{n}\sum_{i=1}^{n}\frac{(p_{a,i}-p_{p,i})}{p_{a,i}}\times 100\%$
	R^2	Indicates the impact of the linear relationship between model predictions and actual values.	$1-\frac{\sum_{i=1}^{n}(p_{a,i}-p_{p,i})^2}{\sum_{i=1}^{n}(p_{a,i}-\bar{m})^2}$
Classification models	Accuracy	The proportion of accurate predictions to the total number of predictions.	$ACC=\frac{T_p+T_n}{T_p+F_p+T_n+F_n}$
	Precision	Proportion of actual successes relative to those projected.	$PPV=\frac{T_p}{T_p+F_p}$
	NPV	Measures the probability of a predicted negative outcome being really negative	$NPV=\frac{T_n}{T_n+F_n}$
	Recall	The proportion of true positives to all positive results.	$recall=\frac{T_p}{T_p+F_n}$
	F1-score	The harmonic mean of precision and recall.	$F1=2\times\frac{PPV+Recall}{PPV+Recall}$
	Specificity	The proportion of true negatives relative to the overall number of such instances.	$Specificity=\frac{T_n}{T_n+F_p}$
	FPR	Determines the proportion of false positives to actual negative instances.	$FPR=\frac{\boldsymbol{F_p}}{\boldsymbol{T_n+F_p}}$

precise forecasts in the field of PV power. For instance, an MLP model was developed to forecast Nigeria's solar power potential, and data from over 195 cities was gathered over ten years [115]. The findings demonstrate that the correlation between average solar irradiation and ANN predictions surpassed 90% for the training and testing datasets. This finding provides compelling evidence that the model can precisely forecast solar radiation in regions without solar radiation data. MLPs are resilient to outliers, have shorter computation times, and lower computational costs than other models [116]. The average computation times of MLPs range from 1.21-1.99 seconds compared to 8.73 and 10.02 seconds for LSTM and BiLSTM, respectively. MLPs may provide better results than some ML models, showing lower

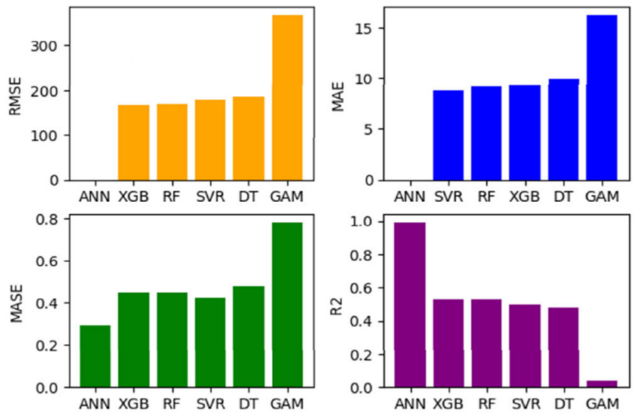

FIGURE 9. Evaluation metrics-based ranking of six ML models [107].

forecasting errors. In [117], the instantaneous thermal efficiency of a solar still is predicted using an MLP and an MLR based on various operational and meteorological variables. Compared to the MLR model, the MLP exhibits superior performance, as evidenced by its 11.23% higher R^2 value and 2.74% lower RMSE values. Similarly, MLP outperforms SVM in predicting solar energy for Oman, with final MSE values of 0.0058 during training and 0.0105 during cross-validation, compared to 0.0263 and 0.0356 for SVM, respectively [118]. Although MLPs are good at capturing complex relationships, they may struggle with temporal data sequences, which may be solved by applying advanced models [21]. In addition, MLPs are unable to address the issue of unstable photovoltaic power in cloudy conditions [119].

To overcome these issues, RNNs provide a notable advancement in managing time-series data, which is essential for forecasting PV power output that is inherently temporal. When applied to time-series data, RNN outperforms ANN in terms of forecasting accuracy, with a notable 26% reduction in RMSE and a significant 47% increase in NMBE [20]. Likewise, an analysis of diverse weather conditions, including sunny, cloudy, and rainy days, [120] reveals that RNN produces the lowest MAPE values, except for the spring season, when compared to two variants of ANN. The average forecasting error of RNN is 7.6%, compared to 20.2% and 10.3% for the other two ANN variants. While training an RNN, significant weather fluctuations may lead to the vanishing or exploding gradient problem, resulting in suboptimal predictions. Researchers developed more advanced RNN variants, such as GRUs and LSTM networks, to solve these limitations. Due to their unique hidden layer architecture, LSTM models can effectively capture short- and long-term temporal relationships in time-series data. On the other hand, GRU shows similar characteristics to LSTM but has the benefit of superior efficiency and less complexity [68]. One study compares the performance of RNN, LSTM, and GRU for solar energy prediction using open-source data. The GRU model has achieved an RMSE value of 289.7 and an MAE value of 151.7, outperforming the LSTM model with values of 396.3 and 222.9 and the RNN model of 450.1 and 275.2. A similar study was conducted in Betul, India, where it was determined that GRU achieved an MAE of 0.03486 and an MSE of 0.00614 [121]. The MAE and MSE values for the LSTM model were slightly higher than those for the GRU, at 0.03659 and 0.00648, respectively, while the RNN model yielded 0.0476 and 0.00802. In contrast, some studies have shown that LSTM has greater accuracy than its alternative, GRU, although it comes with an increased time trade-off [122], [123]. A BiLSTM, another RNN model, may forecast PV power more accurately than LSTM and GRU, as shown in Table 2. Based on data from a meteorological station in Amherst, USA, it was determined that the BiLSTM model predicts solar energy slightly better than the GRU model [124]. The MSE, MAE, and MAPE values for the BiLSTM model were 0.0012, 0.0124, and 12.2%, respectively, whereas the GRU model attained values of 0.0012, 0.0138, and 12.5%. Like BiLSTM, a bidirectional GRU has been proven to be a practical approach for PV power prediction. This approach can provide good forecasting results with reduced computation costs.

Along with RNN, some researchers use CNNs for time series prediction due to their global sharing and local connection capabilities, which may drastically decrease model training parameters and time [125]. In addition, CNNs can successfully manage noisy time series data by reducing noise at each successive layer, resulting in a hierarchical structure of important features and extracting just the relevant ones [24]. For instance, a temporal-CNN (TCNN) is developed to analyze time series data and estimate PV power production [24]. The proposed TCNN's performance is compared to that of FFNN, RNN, LSTM, and GRU. The TCNN achieved the lowest MAE values of 70.015 and 0.510 and the lowest RMSE values of 98.118 and 0.721 for both the University of Queensland and the Sanyo datasets. Another research used TCNN for sequence modelling tasks and assessed its performance using several models, including LSTM, SVR, and ARIMAX [126]. However, in this particular scenario, LSTM models exhibit the highest level of accuracy in terms of performance, surpassing all other models over the years and in general. Also, a novel approach called space-time CNN (STCNN) is introduced, which integrates spatial and temporal convolutional processes inside a single framework [127]. This approach implicitly captured the presence of clouds and their movement without relying on a complex framework. The STCNN achieves the lowest MAPE across all three locations, with a minimum value of 3.98% in California. In comparison, LSTM and FNN achieve MAPE values of 4.25% and 5.15%, respectively. Two novel CNNs, ResNet and DenseNet, are proposed for day-ahead PV power forecasting [128]. DenseNet outperforms other models such as MLP, CNN, and ResNet over a wide range of meteorological conditions and achieves the highest accuracy on the overall testing dataset, as shown in Table 2.

B. HYBRID MODELS

1) HYBRID ANN-METAHEURISTIC MODELS

Hybrid models have gained significant attention due to their notable efficiency in PV power forecasting [146]. A standalone ANN model combined with a metaheuristic optimization algorithm (MOA) can improve predicting accuracy and convergence rate [147]. Table 3 presents a detailed review of ANN models optimized using MOA. MOAs provide a precise and effective technique for exploring the solution space, allowing the model to locate the best parameter combinations. Research has shown that suitable hyperparameter optimization can enhance the model's overall performance by 8% [148]. Fine-tuning the hyperparameters using advanced optimization approaches improves MLP's performance accuracy. Reference [149] proposed an MLP based on grey wolf optimization (GWO) for PV power forecasting, and the model's performance was validated using data from a five kWp PV system. The GWO-MLP model demonstrates the lowest NMAE error of 2.267%, outperforming the particle swarm optimization (PSO)-based MLP (2.532%), levenberg–marquardt (LM)-based MLP (19.995%), and adaptive neuro-fuzzy (ANF)-based MLP (5.112%). As shown in Table 3, the performance of GWO-MLPs is compared with MLPs based on two advanced optimization algorithms: ant-lion optimization (ALO) and whale optimization algorithm (WOA). [150]. The GWO-MLP model, which used the sigmoid activation function, produced the most accurate predictions, with a MAPE of 2.598%. Another study proposes a gray-updated deer hunting optimization algorithm (GU-DHOA) combined with an MLP to predict solar irradiation [151]. The proposed GU-DHOA-MLP performs superior to MLP, with a 22.1% improvement in the RMSE measure. It also outperforms PSO-MLP by 39.7%, WOA-MLP by 12.06%, GWO-MLP by 12.4%, and DHOA-MLP by 12.09%.

Similar to MLPs, the prediction accuracy of RNN and other variants, such as GRU and LSTM, can be increased using a suitable optimization technique. LSTM has superior capability in addressing the vanishing gradient issue and demonstrates improved performance when handling large datasets compared to GRU. Conversely, GRU shares similar characteristics with LSTM but possesses an advantage in high efficiency and reduced complexity.(..)()() [68]. For instance, on the Moroccan city of Fes dataset, RNN, LSTM, and GRU models are optimized using the genetic algorithm (GA) [152]. The findings suggest that the GA-LSTM model outperforms the GA-GRU and GA-RNN models during the summer season. However, the GA-GRU model demonstrates superior performance in the spring and fall seasons compared to the GA-LSTM model. Another research found similar results when three single ANN models—DNN, LSTM, and GRU—were optimized using GA to predict a solar farm's output four hours in advance [153]. With an RMSE of 7.83%, GA-GRU outperformed GA-LSTM (7.92%) and GA-DNN (8.88%). On the other hand, after t+6 time steps, GA-LSTM performed better and produced the lowest RMSE. Another research used an attention mechanism to improve the performance of GA-optimized LSTM [154]. Nevertheless, GA is an outdated optimization technique, and more sophisticated optimization algorithms are employed for LSTM and GRU. When LSTM is optimized using a salp swarm algorithm (SSA) [155], the findings indicate that, compared to XGBoost and LSTM, the MAE decreased by 65.5% and 54.8%, and the RMSE decreased by 74.3% and 62.5%, respectively. In [156], eight advanced MOAs are used to optimize the hyperparameters of LSTM models. This optimization process is performed using four datasets obtained from four turbines located in France. At station 2, the proposed heap-based optimizer (HBO) yielded the most optimal outcomes, with SSA, SCA, GA, DE, GWO, and PSO following in terms of performance. In another study, the authors used a hybrid reptile search algorithm (HRSA) to optimize the hyperparameters of both LSTM and BiLSTM models [157]. The results were compared to seven other robust MOAs, including RSA, SSA, SCA, artificial bee colony (ABC), firefly algorithm (FA), harris hawks optimization (HHO), and chimp optimization algorithm (ChOA). The LSTM model, optimized by HRSA, showed good performance, with an R^2 value of 0.604139 and normalized MAE, MSE, and RMSE values of 0.074450, 0.013668, and 0.116910, respectively. Reference [158] utilizes the same set of seven advanced algorithms to determine the performance levels of a novel boosted self-adaptive (BSA-SCA) method for both LSTM and GRU. The findings indicate that the LSTM approach is marginally superior to the GRU approach in forecasting PV power production. The LSTM-BSA-SCA achieves a R^2 value of 0.617, MAE of 392.801, and RMSE of 620.407, while the GRU-BSA-SCA achieves a R^2 value of 0.613, MAE of 407.445, and RMSE of 623.335. A new approach that integrates ISCA-GRU with partial least-squares analysis (PLS) and complete ensemble empirical mode decomposition (CEEMD) is proposed [159]. The CEEMD-PLS-ISCA-GRU model outperformed eight other comparison models on four datasets.

Similar to LSTM and GRU, optimizing CNN hyperparameters can significantly enhance its accuracy compared to a standard CNN. A CNN and SSA are used to improve the forecasting accuracy of a 500 kWp solar power facility in south Taiwan [160]. Initially, CNN classification was used to categorize past PV power and meteorological data into five weather types. Then, SSA is applied to fine-tune the parameters of these classifications. The CNN-SSA approach demonstrated superior results, with the lowest MRE and MAPE values across all-weather types, particularly in cloudy weather; the CNN-SSA attained a MAPE of 12.25%, surpassing the performance of LSTM-SSA (21.56%) and SVM-SSA (16.25%). Another study demonstrates that GU-DHOA-CNN outperforms CNN, PSO-CNN, WOA-CNN, GWO-CNN, and DHOA-CNN in predicting solar irradiance across multiple performance criteria [151]. Based on

TABLE 2. Summary of standalone ANNs models for PV power forecasting.

Horizon	Time Step	Models	Description	Country	MAE	RMSE	R^2	MAPE	Ref
1 year	10 min	Sandia	Compared Sandia National Laboratories, MLP, and regression methods for estimating power in a microgrid-integrated PV installation.	Italy		34.78 W	0.9858	9.13%	[113]
		Regression				19.71 W	0.9906	5.17%	
		ANN				**17.56 W**	**0.9926**	**4.40%**	
1 day	5 min	LR	Examined the predicted PV power output in Medellín, Colombia, using four supervised learning algorithms: KNN, LR, ANN, and SVM.	Colombia	8.9632 W	94.583 W			[108]
		SVM			9.6209 W	93.644 W			
		KNN			8.8279 W	92.857 W			
		ANN			**8.409 W**	**86.466 W**			
1 hour	1 hour	CHAID	Compared six ML models, including ANN, SVM, RNN, classification and regression tree (CART), chi-square automatic interaction detection (CHAID), and random forest (RF), to predict hourly PV power production.	South Korea		0.98 kW		47.21%	[129]
		SVM				0.83 kW		39.27%	
		CART				0.76 kW		40.08%	
		ANN				0.76 kW		33.72%	
		RF				0.75 kW		33.54%	
		RNN				**0.51 kW**		**23.79%**	
1 day	1 hour	Persistence	Proposed a robust MLP model for predicting PV power in advance, using a pseudo-Huber loss function to address the limitations of a generic MLP.	United States	0.0474 kW	0.0978 kW			[130]
		Generic-MLP			0.0459 kW	0.0788 kW			
		Robust-MLP			**0.0439kW**	**0.0775 kW**			
1 day	1 hour	MLP	Three ML models, namely SVM, MLP, and LSTM, are proposed for forecasting load demand and PV power production.	Australia	10.68 kW	18.37 kW			[131]
		SVM			9.13 kW	14.67 kW			
		LSTM			**8.66 kW**	**14.04 kW**			
1 day	5 min	Persistence	Proposed using an LSTM model with varying layers and nodes to anticipate PV power production for a large-scale power facility in Vietnam.	Vietnam	7.401 MW	11.325 MW		15.42%	[132]
		ARIMA			3.518 MW	5.41 MW		7.33%	
		DRM			3.011 MW	4.415 MW		6.27%	
		MLP			2.546 MW	4.2 MW		5.30%	
		LSTM			**1.676 MW**	**3.082 MW**		**3.49%**	
30 min	5 min	MLP	LSTM outperforms MLP in forecasting daily power production, particularly during low-power periods in the winter.	Canada	600.17 kW	799.9 kW	0.999	2.17%	[21]
		LSTM			**236.3 kW**	**317.4 kW**	**0.9381**	**4.16%**	
15 min 30 min 45 min 60 min 75 min 90 min	15 min	Persistence	Proposed a novel RNN to find nonlinear features and invariant patterns in neighbouring and intra-day datasets. Also, a novel point prediction model is introduced utilizing PV power data without meteorological data.	Belgium	35.15 MW	58.56 MW		17.67%	[133]
		RBF			20.23 MW	30.48 MW		11.79%	
		BPNN			17.49 MW	26.72 MW		9.91%	
		SVM			17.78 MW	23.3 MW		10.95%	
		LSTM			13.87 MW	23.18 MW		7.74%	
		RNN			**10.51 MW**	**17.7 MW**		**6.33%**	
5 min 30 min 60 min	1 min	NAR	Compare the LSTM model with two classical algorithms, the autoregressive neural network (NAR) and the elman recurrent neural network (ENN).	Italy	0.1 kW	0.25 kW	0.97		[134]
		ENN			0.067 kW	0.21 kW	0.98		
		LSTM			**0.054 kW**	**0.16 kW**	**0.99**		
24 hours	1 hour	ELM	LSTM NN and synthetic irradiance prediction are proposed for solar power forecasting, which enhances accuracy by 33% and 44.6% over typical hourly and daily sky forecasts, respectively.	United States	1.38 MW	2.41 MW		284.85 %	[135]
		GRNN			0.67 MW	1.31 MW		34.06%	
		RNN			0.47 MW	0.92 MW		28.79%	
		LSTM			**0.36 MW**	**0.71 MW**		**22.31%**	
10 min	1 min	Persistence	The LSTM model outperforms other models in estimating solar power output at a 1-minute interval, achieving a skill score of 21% RMSE under overcast conditions.	Japan	51.7 W	94.2 W			[136]
		MLP			45.8 W	85..4 W			
		CNN			41.2 W	83.6 W			
		LSTM			40.8 W	82.8 W			
		LSTM-Full			**36.1 W**	**76.9 W**			
5 min	5 min	CNN	Applied univariate and multivariate LSTM models to forecast PV power prediction. Also examined different input variables and forecasted time steps.	Morocco	75.41 W	103.05 W	0.966		[137]
		MLP			43.58 W	69.66 W	0.985		
		LSTM			**28.9 W**	**60.58 W**	**0.99**		
1 hour 2 hours 3 hours	1 hour	ANN	The impact of cloud coverage rates on solar power forecasts was examined, and ANN, LSTM, and GRU were used to validate the proposed methods.	Taiwan	0.035 kW	0.072 kW		9.15%	[138]
		LSTM			0.035 kW	0.067 kW		10.65%	
		GRU			0.029 kW	0.055 kW		**9.02%**	
1 day	60 min	ANN	Studied ANN, LSTM, and GRU for PV power prediction models using various meteorological data.	Taiwan	1.33 kW	1.55 kW		24.0%	[139]
		GRU			0.83 kW	0.89 kW		20.0%	
		LSTM			**0.71 kW**	**0.83 kW**		**16.0%**	
1 hour	1 hour	RNN	Standard RNN, LSTM, and GRU—were tested for PV power forecasting. LSTM and GRU performed better after hyperparameter adjustment.	Romania	275.2 W	450.1 W	0.9648		[140]
		LSTM			222.9 W	396.3 W	0.9727		
		GRU			**151.7 W**	**289.7 W**	**0.9854**		
-	1 hour	RNN	RNN, three univariant LSTM models, and GRU are used to predict PV and wind power output and power consumption.	Spain	0.065 MW	0.98 MW		1.95%	[141]
		BiLSTM			0.043 MW	0.61 MW		1.44%	
		GRU			0.042 MW	0.6 MW		1.40%	
		Stacked-LSTM			**0.025 MW**	**0.4 MW**		**0.67%**	
1 hour	15 min	SARIMA	Proposed a BiLSTM for a 100 MW power plant under different environmental scenarios. The data used is from the rainy days.	Pakistan		25.45 MW	0.48		[142]
		LSTM				0.157 MW	0.91		
		BiLSTM				**0.12 MW**	**0.95**		
1 day	15 min	GRU	An improved BiGRU model is developed by including the bifacial correction coefficient to predict the power output of Bi-PVM accurately.	China	0.56 MW	0.758 MW			[143]
		BiGRU			0.418 MW	0.571 MW			
		Imp. BiGRU			**0.388 MW**	**0.506 MW**			
1 day	15 min	SVR	Focused on developing a microgrid system that utilizes weather data with a CNN for improved	China		53.05 W		6.49%	[144]
		ANN				40.50 W		4.72%	

TABLE 2. ***(Continued.)*** **Summary of standalone ANNs models for PV power forecasting.**

		DBN	Building-Integrated Photovoltaic (BAPV) system performance.			34.78 W	4.21%	
		CNN				**32.66 W**	**3.91%**	
30 min	1 min	NN	Introduced a TCNN model for sequential modelling that integrates causal and dilated convolutions with residual connections. The results shown are from the University of Queensland (UQ).	Australia	75.20 kW	101.69 kW		[24]
		RNN			74.69 kW	102.99 kW		
		LSTM			74.40 kW	101.19 kW		
		GRU			74.27 kW	100.98 kW		
		TCNN			**70.02 kW**	**98.12 kW**		
1 day	1 hour	MLP	Introduced PVPNet, a powerful CNN model for PV power forecasting. The proposed approach generates 24-hour predictions using probabilistic and deterministic methods based on weather data.	Taiwan	196.68 W	224.99 W		[145]
		DT			140.31 W	206.62 W		
		SVM			147.38 W	185.23 W		
		RF			116.01 W	167.53 W		
		LSTM			124.06 W	164.19 W		
		PVPNet			**109.48 W**	**163.15 W**		

a learning percentage of 85, the proposed GU-DHOA-CNN outperforms DHOA-CNN by 7.8%, GWO-CNN by 10.2%, PSO-CNN and WOA-CNN by 8.8%, and CNN by 22.2%. Also, a hybrid algorithm (GA-PSO) is used to optimize the CNN's structure and parameters [161]. This enables the simultaneous achievement of the optimal network structure and connection weight. The hybrid GA-PSO may mitigate the impact of improper hyperparameters and reduce manual modification requirements [26]. The proposed method reduces the MAE by 0.1463 MJm^2 compared to a standalone CNN model. Furthermore, it decreases the annual MAE by 20.34%, 49.47%, and 47.6%, respectively, compared to ANN, K-means-RBF, and GBRT.

2) HYBRID ANN-ANN MODELS

Several research studies have combined multiple ANN models to increase pattern recognition capabilities. Table 3 presents a comparison of various hybrid models to standalone models. In [124], three RNN variants—GRU, LSTM, and BiLSTM—are used to assess six distinct combinations for predicting solar energy using data from a meteorological station in Amherst, USA. LSTM-BiLSTM outperformed other combinations in three out of five time steps, with the lowest MSE, MAE, and RMSE values obtained at timestep 24 of 0.001636, 0.018218, and 0.04045, respectively. Advanced hybrid models are also introduced to assess the influence of combining CNNs with three RNN models: LSTM, BiLSTM, and GRU. For instance, [162] proposed a hybrid approach that integrates attention mechanisms, CNN, LSTM, and clustering techniques with wireless sensor networks to address the prevailing challenges associated with the predictions of PV power production. The proposed approach achieves low RMSE, MAPE, and MAE values, particularly at a timestep of 7.5 minutes. Another study introduced a hybrid model using five convolutional layers and three recurrent layers [148]. The data analysis revealed that the 5CNN-3LSTM model outperformed the 5CNN-3GRU and 5CNN-3BiLSTM models by 3.2% and 1.3%, respectively, in terms of MSE. The CNN model had the lowest forecasting performance across a 24-hour prediction horizon, but when merged with BiGRU, the hybrid model had the highest accurate findings [163]. The MAPE value of the BiGRU-CNN is 3.42%, which is lower than the MAPE values of 5.58% for the CNN and 4.10% for the GRU. Similarly, a hybrid approach is proposed using an improved BiGRU model, CNN layer, and attention mechanism to improve PV power prediction [164]. The proposed CNN-BiGRU performs better than a single model and other hybrid models across various weather conditions. The RMSE value for the CNN-BiGRU model is 4.921, which is lower than the RMSE values of 5.302 for CNN-BiLSTM, 5.277 for CNN-BiRNN, 6.597 for SVM, and 5.722 for TCNN. Some studies have combined the characteristics of three different ANN models into one model, while others use an MOA to optimize the hybrid ANN-ANN models, as shown in Table 3. In [165], a combination of WPD and three single models (CNN, LSTM, and MLP) is proposed to achieve the hour-ahead forecast of solar irradiation. The experimental findings obtained from the Denver, Clark, and Folsom datasets demonstrate superior predictive accuracy compared to other models. The RMSE value obtained is 32.1, the normalized RMSE is 15.4795%, and the skill score (s) reaches a maximum of 0.4438. Similarly, a DNN-RNN hybrid model is optimized for optimum performance using the slow rider-based rider optimization algorithm (S-ROA) [166]. The S-ROA-DRNN outperformed other learning algorithms such as PSO, WOA, GWO, and ROA. Reference [111] also proposes a hybrid technique SSA-RNN-LSTM for one-hour PV power forecast for three PV systems: polycrystalline, monocrystalline, and thin-film. SSA-RNN-LSTM performance is then compared against RNN-LSTM, GA-RNN-LSTM, and PSO-RNN-LSTM. The proposed approach showed lower testing errors (RMSE and MAE) than RNN-LSTM for polycrystalline, monocrystalline, and thin-film PV systems. Notably, the reductions in errors were 19.14% and 21.57%, 15.4% and 10.81%, and 22.9% and 25.2% for the corresponding PV systems. Table 3 presents a detailed summary of various hybrid models for PV power forecasting. First, ANN models are combined with multiple MOAs, then different combinations of ANN models are compared, and lastly, hybrid models optimized with MOAs are compared. The models highlighted are the top performers among the models.

TABLE 3. Summary of standalone ANNs models for PV power forecasting.

Horizon	Time Step	Models	Description	Country	MAE	RMSE	R^2	MAPE	Ref
1 hour 2 hour	1 hour	Persistent	Examined different models to predict PV power production in Merced, California. The ANN optimized with GA performs better than other models.	California	91.12 kW	160.79 kW	0.83		[167]
		ARIMA			102.76 kW	144.26 kW	0.86		
		kNN			87.76 kW	162.37 kW	0.82		
		ANN			89.12 kW	142.74 kW	0.86		
		GA-ANN			**62.53 kW**	**104.28 kW**	**0.93**		
1 day	1 day	ALO-MLP	A GWO, ALO, and WOA-based MLP model for PV power was proposed. This also studied how inputs and activation functions impacted forecasting accuracy.	Australia	0.068 kW		0.7101	12.11%	[150]
		WOA-MLP			0.05 kW		0.8362	7.32%	
		GWO-MLP			**0.017 kW**		**0.9791**	**2.60%**	
30 min	30 min	XGBoost	Proposed a hybrid approach that integrates LSTM and PSO to improve the precision of PV power forecasts using time series data.	-	16.35 MW	32.47 MW			[168]
		ANN			11.26 MW	22.79 MW			
		LSTM			8.54 MW	19.15 MW			
		PSO-LSTM			**6.68 MW**	**15.49 MW**			
-	5 min	LSTM	The proposed ICHOA-GRU improves the basic CHOA algorithm's optimization and iteration performance using elite reverse learning and adaptive mutation.	Australia	0.2162 kW	0.2605 kW	0.9739		[169]
		GRU			0.1021 kW	0.1629 kW	0.989		
		PSO-GRU			0.0972 kW	0.1531 kW	0.9903		
		CHOA-GRU			0.0907 kW	0.1528 kW	0.9913		
		ICHOA-GRU			**0.0742 kW**	**0.1028 kW**	**0.9956**		
5 min	5 min	LSTM	GA-BiLSTM outperforms other models in 5-minute ahead PV power forecasts, even in the absence of weather data, with the lowest RMSE value of 0.438.	China	0.243 kW	0.243 kW	0.981		[170]
		ELM			0.345 kW	0.345 kW	0.962		
		BPNN			0.439 kW	0.439 kW	0.937		
		GA-BPNN			0.253 kW	0.253 kW	0.976		
		PSO-BiLSTM			0.282 kW	0.282 kW	0.981		
		GA-BiLSTM			**0.242 kW**	**0.242 kW**	**0.983**		
1 week	5 min	LSTM-RNN	The hybrid GRU-RNN outperforms the LSTM-RNN marginally in weekly PV power forecasting.	Australia	2.26 W	3.38 W		0.17%	[146]
		GRU-RNN			**2.12 W**	**3.02 W**		**0.84%**	
10 min	10 min	5D-LSTM	Proposed a CNN-LSTM model with five layers to capture local information and temporal patterns.	México	0.16667 W	0.29237 W			[171]
		2D-CNN-LSTM			0.14106 W	0.24298 W			
		5D-CNN-LSTM			**0.05193 W**	**0.08305 W**			
24 hours	1 hour	CNN	Proposed a hybrid AE-GRU model that employs a sequence-to-sequence auto-encoder (AE) to discover internal connections and reduce reconstruction error and a GRU to capture temporal relationships.	India	0.0693 W		0.9396		[172]
		LSTM			0.0325 W		0.9546		
		GRU			0.0321 W		0.9242		
		CNN-LSTM			0.0341 W		0.8976		
		CNN-GRU			0.0387 W		0.8877		
		AE-GRU			**0.0277 W**		**0.93761**		
1 hour		CNN	DSCLANet, which includes a dual-stream CNN, an LSTM, and a self-attention mechanism (AM), is proposed. The proposed model uses a self-AM and spatial and temporal feature vector fusion to select ideal features.	Australia	0.1526 kW	0.3108 kW			[173]
		LSTM			0.143 kW	0.2836 kW			
		GRU			0.1518 kW	0.2912 kW			
		CNN-LSTM			0.12 kW	0.2606 kW			
		CNN-GRU			0.1519 kW	0.2817 kW			
		DSCLANet			**0.0632 kW**	**0.1291 kW**			
-	5 min	RNN-LSTM	Proposed a hybrid model that integrates CNN, BiLSTM, and AM to capture temporal relationships effectively. The hyperparameters of the proposed model are optimized using Bayesian optimization.	India	0.4583 kW				[174]
		RNN-BiLSTM			0.4202 kW				
		GRU-LSTM			0.4703 kW				
		CNN-LSTM			0.4661 kW				
		CNN-BiLSTM			**0.4265 kW**				
-	5 min	LSTM	The proposed model utilizes LSTM to capture temporal information and CNN to capture spatial features.	Australia	0.327 kW	0.709 kW		0.062%	[125]
		CNN			0.304 kW	0.822 kW		0.058%	
		CNN-LSTM			0.294 kW	0.693 kW		0.056%	
		LSTM-CNN			**0.221 kW**	**0.621 kW**		**0.042%**	
1 hour	5 min	CNN-LSTM	CNN-assisted deep echo state network (CNN-DeepESN) and principal components analysis (PCA) are proposed to solve PV power generation's unpredictable`` nature.	Australia	0.294 kW	0.693 kW		5.40%	[175]
		LSTM-CNN			0.221 kW	0.621 kW		4.20%	
		CNN-DeepESN			**0.038 kW**	**0.310 kW**		**3.33%**	
-	5 min	RNN	Proposed a hybrid model that combines the BiLSTM and CNN structures, using the BiLSTM for temporal information and the CNN for spatial features.	Australia	0.2706 kW	0.3191 kW	0.9921		[176]
		LSTM			0.2531 kW	0.2812 kW	0.9938		
		GRU			0.1752 kW	0.2016 kW	0.9968		
		CNN			0.1325 kW	0.1798 kW	0.9975		
		BLSTM			0.129 kW	0.1609 kW	0.9979		
		CNN–LSTM			0.1064 kW	0.1389 kW	0.9985		
		LSTM–CNN			0.0794 kW	0.1102 kW	0.999		
		BLSTM–CNN			**0.0531 kW**	**0.0944 kW**	**0.9993**		
15 min	15 min	BagTree	Proposed an advanced multivariate model for predicting solar output, which incorporates variational mode decomposition (VMD), CNN, and BiGRU. Each sub-mode of the PV power series is decomposed using	Korea	1.75 MW	2.36 MW	0.87	22.85%	[177]
		ANN			1.68 MW	2.28 MW	0.875	21.85%	
		GRU			1.62 MW	2.24 MW	0.879	21.11%	
		CNN-ANN			1.57 MW	2.19 MW	0.891	20.44%	
		BiGRU			1.51 MW	2.15 MW	0.89	19.64%	
		CNN-BiGRU			1.49 MW	2.1 MW	0.9	19.43%	

TABLE 3. ***(Continued.)*** **Summary of standalone ANNs models for PV power forecasting.**

		EEMD-CNN-BiGRU	VMD and predicted using a CNN-BiGRU framework using prior PV power values and other weather-related variables.		0.74 MW	1.03 MW	0.975	9.64%	
		VMD-BiGRU			0.34 MW	0.47 MW	0.995	4.46%	
		VMD-CNN-BiGRU			**0.3 MW**	**0.4 MW**	**0.996**	**3.86%**	
1 hour	1 hour	GCVCNN-BiGRU	Introduced a hybrid model (CNN-MRNN) that was fine-tuned using GridSearchCV to provide accurate PV and wind power forecasts.	China	0.036 MW	0.0782 MW	0.9348		[178]
		CNN-LSTM			0.0345 MW	0.07231MW	0.9465		
		CNN-BiLSTM			0.0315 MW	0.0707 MW	0.9487		
		GCVCNN-RNN			0.0215 MW	0.0423 MW	0.9677		
		GCVCNN-MRNN			**0.0153 MW**	**0.0168MW**	**0.9844**		
24 hours	15 min	CNN	Introduced an integrated model that optimizes CNN-LSTM hyperparameters using the coati optimization algorithm (COA) for wind and PV power predictions.	China	0.0274 MW	0.024 MW	0.9519		[179]
		LSTM			0.0239 MW	0.0174 MW	0.9611		
		PSO-CNN-LSTM			0.0218 MW	0.0194 MW	0.9676		
		GWO-CNN-LSTM			0.0199 MW	0.018 MW	0.9665		
		COA-CNN-LSTM			**0.0174 MW**	**0.014 MW**	**0.9815**		

V. RESULTS AND DISCUSSIONS

PV power forecasting is used to enhance the efficiency of the power system and streamline power exchange. Various methods, including physical, statistical, AI, and hybrid techniques, have been developed to enhance forecasting accuracy. However, ANNs are notable for their exceptional performance and efficiency owing to their adaptable nature. These models are highly accurate, analyzing large amounts of data and identifying complex patterns. In addition, ANNs provide real-time predictions to adjust to fluctuating weather conditions, enhancing grid reliability and facilitating more informed decision-making. Over time, advanced ANN models are proposed to increase the accuracy of PV power forecasts for various geographical regions.MLP, RNN, LSTM, GRU, and CNN are widely used models for PV power forecasting due to their unique internal structures and ability to handle large data sets.In standalone models, MLPs are widely known for their ability to handle large datasets and approximate any nonlinear function accurately. However, these models could encounter difficulties when dealing with temporal data sequences [21]. In addition, MLPs are unable to address the issue of unstable photovoltaic power in diverse weather conditions [119]. RNNs have shown promising results in analyzing time-series data, yet standard RNN models still exhibit various constraints. The performance of standard RNN is limited by its short-term memory. When these models are applied to data that show significant fluctuations, it can give rise to the vanishing or exploding gradient problem, leading to suboptimal predictions. In recent years, there has been an increasing interest in using LSTM and GRU models for PV power prediction. These models have gained popularity due to their gate structure, which effectively addresses the limitations of short-term memory. Based on the analysis and the provided list of tables, the GRU has a slight advantage over the LSTM because of its simpler structure. Some studies have shown that LSTM tends to have greater accuracy than its alternative, GRU, although it does come with a trade-off of increased time. In [123], the LSTM model has a slightly lower error rate than the GRU model. However, the GRU model requires less time for training (2.9 hours) and prediction (11.02 seconds) than the LSTM model, which takes 3.27 hours for training and 11.84 seconds for prediction. According to another research study, GRU is 29.29 percent more efficient than LSTM in handling the same data [180]. Hence, considering training time and forecasting accuracy, the GRU model may provide acceptable outcomes for predicting PV power and irradiance [181]. Nevertheless, the difference between the error rates of LSTM and GRU is minimal. By optimizing the parameters correctly, the performance may be enhanced even more. Although LSTM and GRU models have shown promising results for PV power forecasting, it is important to note that these models only consider unidirectional data input. BiLSTM and BiGRU models have recently demonstrated significant nonlinear fitting capacity and robust mapping proficiency in forecasting across several domains. BiLSTM and BiGRU, as opposed to unidirectional LSTM and GRU, simultaneously process the sequence in both forward and backward directions. Thus, these models may outperform their unidirectional counterparts. The comparison of BiLSTM and BiGRU with their unidirectional counterparts, LSTM and GRU, is shown in [142] and [143]. Reference [182] showed that the RMSE values for BiGRU, BiLSTM, GRU, and LSTM are 46.3937, 46.4137, 47.0531, and 47.1504, respectively. According to multiple studies, BiGRU models have a modest advantage over BiLSTM models regarding forecasting accuracy [182], [183]. Traditional CNN has shown promising results for time series data, but its performance is still lower than LSTM and GRU, as demonstrated in Table 2. CNNs are effective at processing spatial data and identifying static patterns. On the other hand, RNNs, LSTMs, and GRUs are more suitable for predicting time series that include temporal relationships. However, recent variants of CNN, such as TCNN, DenseNet, Resnet, and others, exhibit superior performance compared to RNN, LSTM, and GRU. Fig.10 compares the TCNN, ResNet, and DenseNet with different machine learning models.

Different combinations are presented in hybrid models; almost all indicate that hybrid models outperform single models, as shown in Table 3. Some studies used ANN models with metaheuristic algorithms to improve forecasting accuracy. For instance, ANN is optimized using PSO to predict daily solar radiation for several sites in Saudi Arabia [184].

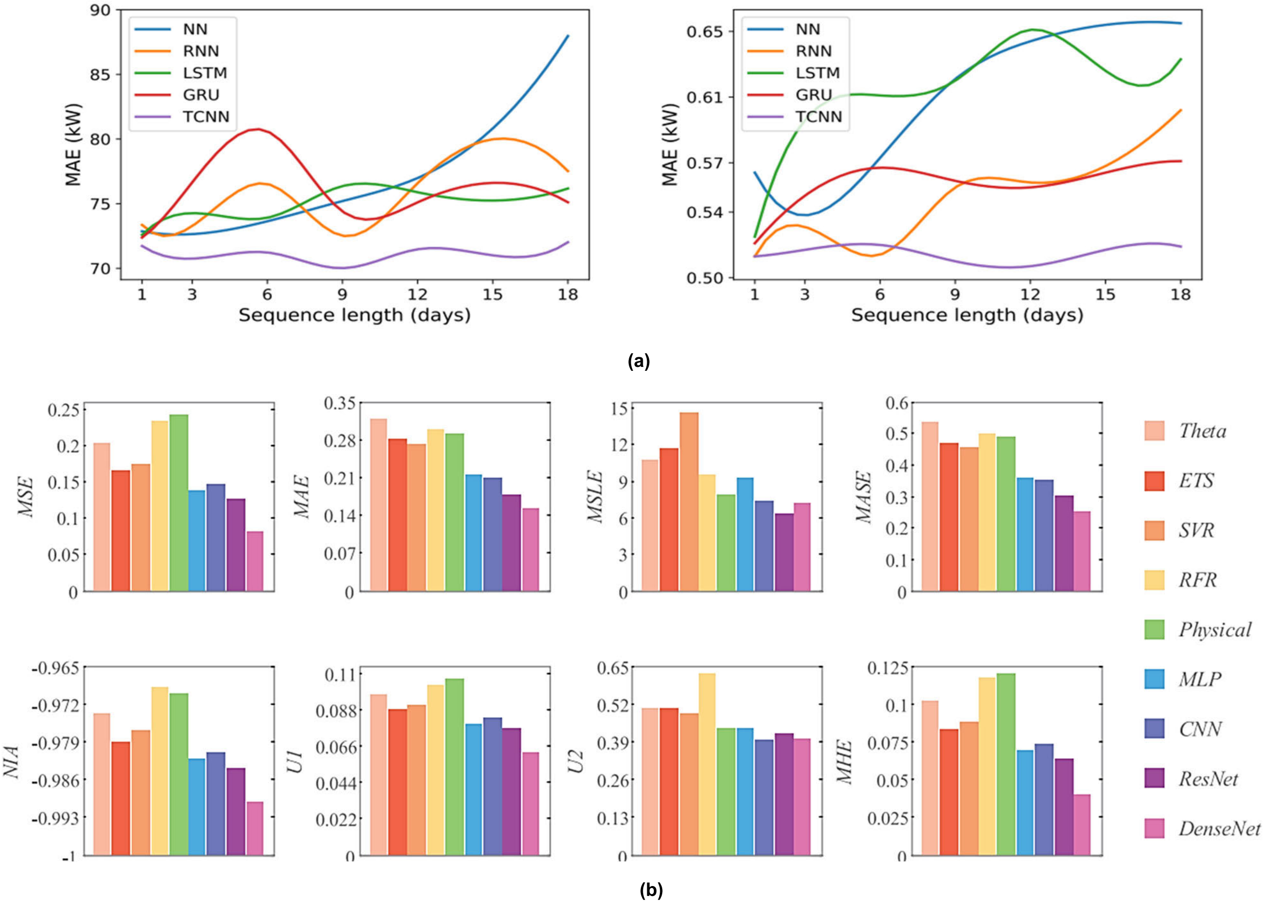

FIGURE 10. **Comparison between different variants of CNN and ML models (a) TCNN [24] (b) DenseNet and ResNet [128].**

The PSO-ANN performed better than the BP-ANN, with a mean MAPE of 8.85% compared to 12.61% for the BP algorithm. GA, another commonly used optimization algorithm, may outperform PSO when addressing complex optimization problems [170]. However, GA and PSO are outdated optimization techniques, and more advanced algorithms are used to optimize ANN models. The shuffled frog leaping algorithm (SFLA) and gradient descent are used to optimize ANN hyperparameters. The MAPE value for Oviedo using the proposed method is 8.8%, lower than the standard SFLA-ANN (9.57%) and GA-ANN (9.92%) models. In another research, HBO produced the most optimal outcomes, with SSA, SCA, GA, DE, GWO, and PSO following in terms of performance using four datasets obtained from four turbines in France [156]. Similarly, a hybrid algorithm HRSA is used to optimize the hyperparameters of LSTM and BiLSTM models, and the outcomes are compared with seven advanced MOAs [157]. The HRSA hybrid showed the most favourable outcomes, with FA, HHO, RSA, SCA, ABC, SSA, and ChOA following suit in assessing their effectiveness for both LSTM and BiLSTM models. Reference [158] uses the same seven advanced algorithms to evaluate the performance of the novel BSA-SCA approach for both LSTM and GRU. The BSA-SCA algorithm outperforms other algorithms, with RMSE and MAE values of 620.407 and 392.801 for LSTM and 623.335 and 407.445 for GRU, respectively. However, in this case, in terms of performance, the proposed approach is followed by SCA, while the FA and RSA show the lowest performance on multiple metrics.

Various studies have integrated several ANN models to improve pattern recognition capability. CNN-LSTM is a commonly used model in literature for predicting PV power and irradiance. CNNs excel in analyzing and interpreting spatial data, but LSTMs are better suited for forecasting time series that include temporal dependencies. Fig. 11 demonstrates that CNN-LSTM is superior in performance in three different weather circumstances since it offers a higher frequency of performance. However, multiple studies have concluded that LSTM-CNN outperforms CNN-LSTM regarding forecasting accuracy [125], [176]. According to one study, BiLSTM-CNN is a more effective combination of ANN models [176]. The authors found that the BiLSTM-CNN model yields lower RMSE, MAE, MSE, and R^2 values for PV power forecasting compared to the CNN-LSTM and LSTM-CNN models. Another study revealed that the GRU-CNN model

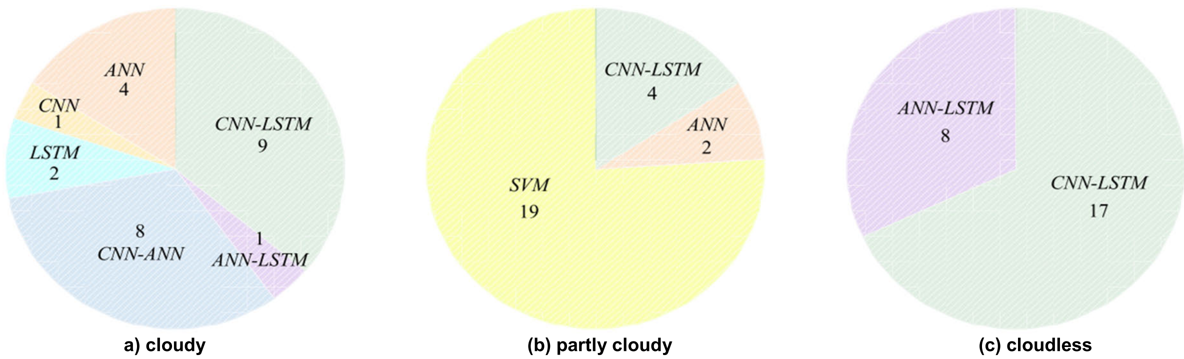

FIGURE 11. Frequency of each model performs best in three weather conditions [186].

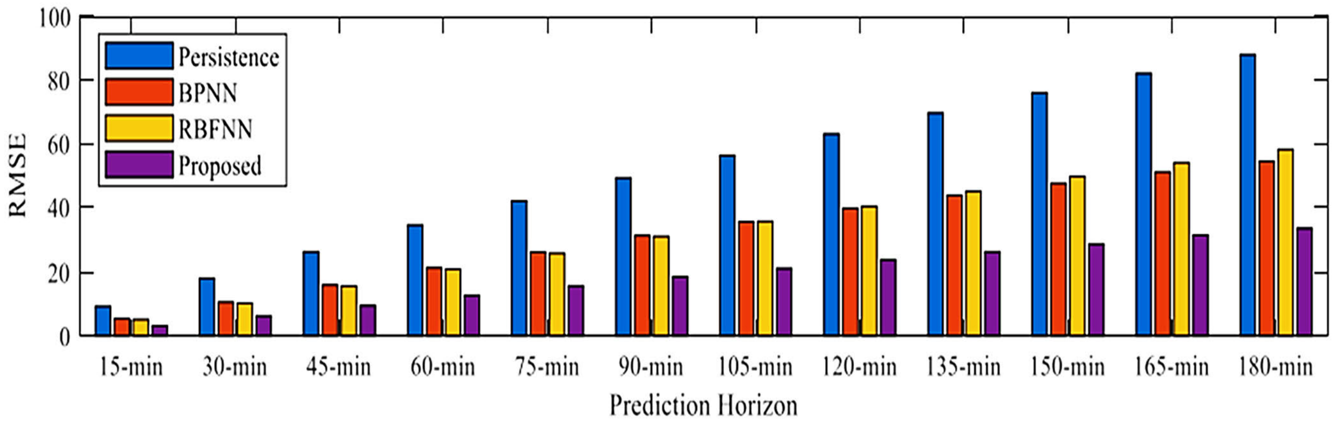

FIGURE 12. RMSE values for different prediction horizons [188].

outperforms CNN-LSTM, CNN-GRU, and LSTM-CNN models on four datasets [185]. The GRU-CNN model (0.2606), and LSTM-CNN model (0.2239). Keeping up with the current trend of hybrid models, [163] proposed a combination of BiGRU and CNN for load forecasting. The BiGRU-CNN model achieves a low MAPE of 3.42% and RMSE of 122.22, which is much better than the GRU-CNN model (MAPE: 14.51%, RMSE: 625.36) and the CNN-BiGRU model (MAPE: 5.10%, RMSE: 196.09). TCN, similar to CNN, may be used with unidirectional and bidirectional LSTM and GRU models. Reference [187] presented a hybrid model that combines a BiGRU and TCN for day-ahead forecasting. The study also compares the results with other models, such as LSTM-TCN, BiLSTM-TCN, GRU-TCN, and BiGRU-TCN. The findings indicate that BiGRU-TCN has the lowest error rate among the different combinations for various datasets.

VI. LIMITATIONS AND SHORTCOMINGS

A precise forecast is essential to achieve higher levels of PV power integration while ensuring cost-effectiveness and economic sustainability. Although PV power forecasting offers many benefits, using ANN models has several limitations. Multiple studies have shown that as the forecasting horizon or timesteps increase, the accuracy of forecasts tends to decrease, regardless of whether standalone or hybrid models are used. In [162], the accuracy of both the standalone and proposed hybrid CNN-LSTM model decreases as the number of timesteps increases. The RMSE of the CNN-LSTM model at a timestep of 7.5 minutes is 1.30. It then decreases to 1.40 and reaches a higher value of 2.04 at a timestep of 30 minutes. This value exceeds the values of the standalone models for 7.5-minute and 15-minute timesteps. In another study [188], the accuracy decreases as the forecasting horizons or prediction windows increase. Expanding the forecasting horizons from 15 minutes to one hour leads to a notable rise in the average MAE error, approximately 3.8 to 4.7 times greater. The error is further increased when the forecasting horizon is set to 120 minutes, with a factor of 7.3-10.4. Fig. 12 illustrates how the RMSE value rises as the prediction windows lengthen during the spring season. In addition, some research has proposed hybrid models for more accurate predictions of PV power production. Nevertheless, hybrid models have shown lower efficiency or a marginal improvement than standalone models. For instance, regarding forecasting accuracy, the standalone GRU model outperforms the hybrid model CuDNNGRU, with an RMSE of 7.83% compared to 7.87% [153]. Additionally,

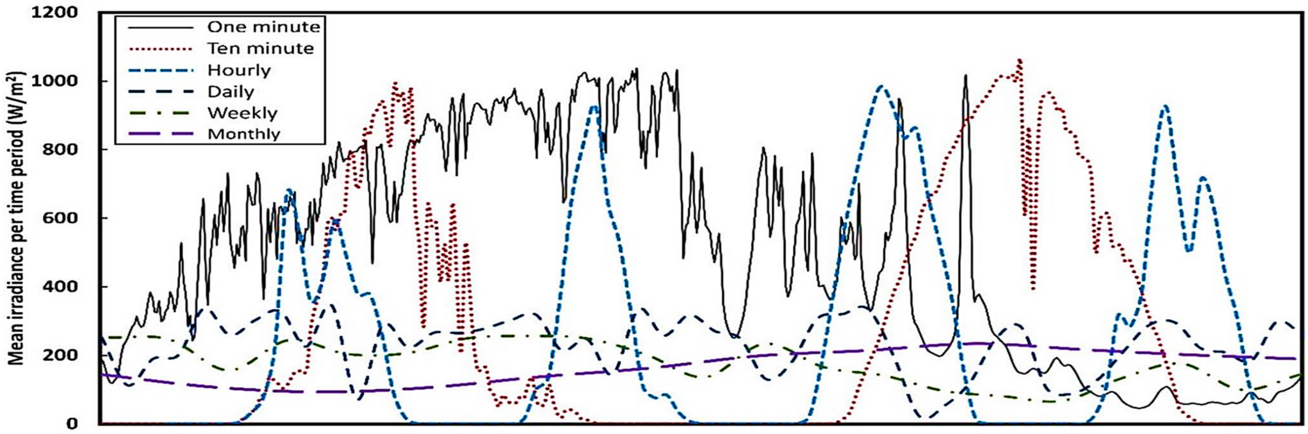

FIGURE 13. Horizontal irradiance fluctuation in South Korea [181].

the complex structure of the hybrid model also presents a challenge, as any malfunction in one model would greatly magnify the difference between the anticipated and actual solar output [146]. Training time is a critical determinant when evaluating the feasibility of PV power forecasting models. Hybrid models require 1.5 to 13.5 times more time to train than single-stage models [125]. The hybrid model has to capture both temporal and spatial information from the dataset [181], leading to an increase in training and running time. These limitations impact the practicality and use of these systems. Another limitation is that the ANN modelling technique relies primarily on weather data as its input. Unpredictable weather conditions might lead to less accurate predictions and unexpected power interruptions. The forecasts' performance may still be inaccurate if any last-minute adjustments occur. Fig. 13 shows the fluctuations in horizontal irradiance in South Korea, both minute-by-minute and hourly. The figure indicates significant fluctuations in irradiance, ranging from over 1000 W/m^2 to below 400 W/m^2 within a one-minute time interval. In addition, these models required a considerable amount of data to provide precise forecasts and reliable generalization. Sometimes, the given data contains noise and missing values, increasing the forecasting error probability. Hence, obtaining high-quality and reliable training data may be challenging [189]. Also, large amounts of high-quality training data enhance the system's computational complexity [190].

VII. CONCLUSION AND FUTURE WORKS

ANN models can enhance PV power forecasting and improve grid stability by assessing data quality and model complexity and conducting rigorous validation. Hence, this paper provides an in-depth review of recent developments in PV power forecasting, specifically focusing on five popular ANN models: MLP, RNN, LSTM, GRU, and CNN. In addition, this study also examines and compares different variants of these models, including BiRNN, BiLSTM, BiGRU, and TCNN. Whether used as a standalone model or in a hybrid configuration, these models offer better forecasting accuracy and shorter training times. However, multiple factors, such as the forecasting period, meteorological conditions, and evaluation metrics, must be considered, which might lead to inaccuracy. It is also important to consider other factors, such as the quality and quantity of data, the suitability of the algorithm, the availability of computational resources, and the complexity of the model when making forecasts for a specific region.

Based on a thorough analysis of both standalone and hybrid models for PV power forecasting, the key findings of this review can be summarized as follows:

➢ Considering standalone models,
  - GRU is more accurate for time series data than LSTM, RNN, CNN, and MLP due to its intrinsic memory capacities. Some studies have shown that LSTM has greater accuracy than its alternative, GRU, although it comes with an increased time trade-off.
  - BiGRU, BiLSTM, and BiRNN models have been found to outperform their unidirectional counterparts.
  - Among bidirectional models, BiGRU has a slight edge over BiLSTM when considering both the computational burden and forecasting accuracy.
  - Advanced versions of CNN models, such as TCNN and DenseNet, have demonstrated superior performance to GRU and LSTM models.

➢ Considering hybrid models,
  - Hybrid models combining CNN with bidirectional and unidirectional GRU and LSTM outperformed other combinations.
  - CNN-LSTM is a popular hybrid model, although studies suggest it is less accurate than LSTM-CNN.
  - Forecasting accuracy is slightly higher when CNN is integrated with BiGRU and GRU than when integrated with BiLSTM and LSTM.

- Overall, BiGRU, combined with CNN or TCNN, leads to superior performance compared to BiLSTM, GRU, and LSTM.
- Similarly, metaheuristic algorithms for hyperparameter tuning increase the forecasting accuracy of standalone and hybrid ANN models
- Among MOAs, hybrid or updated metaheuristic algorithms have produced superior results.

This study presented the results from various studies to support readers in comprehending, categorizing, and comparing the five commonly used ANN models, eventually promoting innovation in this sector. Future research might include reviewing these five ANN models for a specific location to obtain even better review outcomes. Although most research papers applied distinct datasets, it is challenging to assess if a forecasting model may be successful when applied to different types of data. Hence, analyzing the forecasting models using diverse datasets from multiple locations is highly recommended. It is also recommended that important details for the electrical grid be provided, such as upper and lower limits of forecasts and the degree of confidence associated with each statistic.

REFERENCES

[1] S. R. Shakeel, J. Takala, and W. Shakeel, "Renewable energy sources in power generation in Pakistan," *Renew. Sustain. Energy Rev.*, vol. 64, pp. 421–434, Oct. 2016, doi: 10.1016/j.rser.2016.06.016.

[2] R. Asghar, M. H. Sulaiman, Z. Mustaffa, N. Ullah, and W. Hassan, "The important contribution of renewable energy technologies in overcoming Pakistan's energy crisis: Present challenges and potential opportunities," *Energy Environ.*, vol. 34, no. 8, pp. 3450–3494, Dec. 2023, doi: 10.1177/0958305x221134110.

[3] J. L. Holechek, H. M. E. Geli, M. N. Sawalhah, and R. Valdez, "A global assessment: Can renewable energy replace fossil fuels by 2050?" *Sustainability*, vol. 14, no. 8, p. 4792, Apr. 2022, doi: 10.3390/su14084792.

[4] R. Asghar, F. Rehman, Z. Ullah, A. Qamar, K. Ullah, K. Iqbal, A. Aman, and A. A. Nawaz, "Electric vehicles and key adaptation challenges and prospects in pakistan: A comprehensive review," *J. Cleaner Prod.*, vol. 278, Jan. 2021, Art. no. 123375, doi: 10.1016/j.jclepro.2020.123375.

[5] International Energy Agency. *Solar PV*. Accessed: Jan. 2023. [Online]. Available: https://www.iea.org/energy-system/renewables/solar-pv

[6] D. Dudley. (2022). *Solar Overtakes Wind Energy for First Time in Global Rush for Renewables*. Accessed: Apr. 12, 2022. [Online]. Available: https://www.forbes.com/sites/dominicdudley/2022/04/12/solar-overtakes-wind-energy-for-first-time-in-global-rush-for-renewables/

[7] International Energy Agency. (2021). *Net Zero By 2050: A Roadmap for the Global Energy Sector*. [Online]. Available: https://iea.blob.core.windows.net/assets/deebef5d-0c34-4539-9d0c-10b13d840027/NetZeroby2050-ARoadmapfortheGlobalEnergySector_CORR.pdf

[8] Bloomberg News. *Solar May Generate Half of World's Power by 2050*. Accessed: Apr. 20, 2022. [Online]. Available: https://www.bloomberg.com/news/articles/2022-04-20/solar-energy-may-generate-half-of-world-s-power-by-2050#xj4y7vzkg

[9] H. Wang, Y. Liu, B. Zhou, C. Li, G. Cao, N. Voropai, and E. Barakhtenko, "Taxonomy research of artificial intelligence for deterministic solar power forecasting," *Energy Convers. Manage.*, vol. 214, Jun. 2020, Art. no. 112909, doi: 10.1016/j.enconman.2020.112909.

[10] R. Ahmed, V. Sreeram, Y. Mishra, and M. D. Arif, "A review and evaluation of the state-of-the-art in PV solar power forecasting: Techniques and optimization," *Renew. Sustain. Energy Rev.*, vol. 124, May 2020, Art. no. 109792, doi: 10.1016/j.rser.2020.109792.

[11] F. Corti, A. Laudani, G. M. Lozito, M. Palermo, M. Quercio, F. Pattini, and S. Rampino, "Dynamic analysis of a supercapacitor DC-link in photovoltaic conversion applications," *Energies*, vol. 16, no. 16, p. 5864, Aug. 2023, doi: 10.3390/en16165864.

[12] International Renewable Energy Agency, Abu Dhabi, United Arab Emirates. (Jul. 2023). *Renewable Energy Statistics 2023*. [Online]. Available: https://mc-cd8320d4-36a1-40ac-83cc-3389-cdn-endpoint.azureedge.net/-/media/Files/IRENA/Agency/Publication/2023/Jul/IRENA_Renewable_energy_statistics_2023.pdf?rev=7b2f44c294b84cad9a27fc24949d2134

[13] R. Meenal, D. Binu, K. C. Ramya, P. A. Michael, K. V. Kumar, E. Rajasekaran, and B. Sangeetha, "Weather forecasting for renewable energy system: A review," *Arch. Comput. Methods Eng.*, vol. 29, no. 5, pp. 2875–2891, Aug. 2022, doi: 10.1007/s11831-021-09695-3.

[14] S. Ghimire, T. Nguyen-Huy, R. Prasad, R. C. Deo, D. Casillas-Pérez, S. Salcedo-Sanz, and B. Bhandari, "Hybrid convolutional neural network-multilayer perceptron model for solar radiation prediction," *Cognit. Comput.*, vol. 15, no. 2, pp. 645–671, Mar. 2023, doi: 10.1007/s12559-022-10070-y.

[15] B. C. Erdener, C. Feng, K. Doubleday, A. Florita, and B.-M. Hodge, "A review of behind-the-meter solar forecasting," *Renew. Sustain. Energy Rev.*, vol. 160, May 2022, Art. no. 112224, doi: 10.1016/j.rser.2022.112224.

[16] B. Li and J. Zhang, "A review on the integration of probabilistic solar forecasting in power systems," *Sol. Energy*, vol. 210, pp. 68–86, Nov. 2020, doi: 10.1016/j.solener.2020.07.066.

[17] A. Mahrouch, M. Ouassaid, Z. Cabrane, and S. H. Lee, "De-loaded technique enhanced by fuzzy logic controller to improve the resilience of microgrids based on wind energy and energy storage systems," *Energies*, vol. 16, no. 1, p. 291, Dec. 2022, doi: 10.3390/en16010291.

[18] M. Palermo, F. Forconi, E. Belloni, M. Quercio, G. M. Lozito, and F. R. Fulginei, "Optimization of a feedforward neural network's architecture for an HVAC system problem," in *Proc. 3rd Int. Conf. Electr., Comput., Commun. Mechatronics Eng. (ICECCME)*, Tenerife, Spain, Jul. 2023, pp. 1–6, doi: 10.1109/iceccme57830.2023.10252568.

[19] E. Belloni, F. Grasso, G. M. Lozito, D. Poli, F. R. Fulginei, and G. Talluri, "Neural-assisted HVACs optimal scheduling for renewable energy communities," *Energy Buildings*, vol. 301, Dec. 2023, Art. no. 113658, doi: 10.1016/j.enbuild.2023.113658.

[20] Z. Pang, F. Niu, and Z. O'Neill, "Solar radiation prediction using recurrent neural network and artificial neural network: A case study with comparisons," *Renew. Energy*, vol. 156, pp. 279–289, Aug. 2020, doi: 10.1016/j.renene.2020.04.042.

[21] M. Elsaraiti and A. Merabet, "Solar power forecasting using deep learning techniques," *IEEE Access*, vol. 10, pp. 31692–31698, 2022, doi: 10.1109/ACCESS.2022.3160484.

[22] M. Abdel-Nasser and K. Mahmoud, "Accurate photovoltaic power forecasting models using deep LSTM-RNN," *Neural Comput. Appl.*, vol. 31, no. 7, pp. 2727–2740, Jul. 2019, doi: 10.1007/s00521-017-3225-z.

[23] M. Aamir, Z. Rahman, W. Ahmed Abro, M. Tahir, and S. M. Ahmed, "An optimized architecture of image classification using convolutional neural network," *Int. J. Image, Graph. Signal Process.*, vol. 11, no. 10, pp. 30–39, Oct. 2019, doi: 10.5815/ijigsp.2019.10.05.

[24] Y. Lin, I. Koprinska, and M. Rana, "Temporal convolutional neural networks for solar power forecasting," in *Proc. Int. Joint Conf. Neural Netw. (IJCNN)*, Glasgow, U.K., Jul. 2020, pp. 1–8, doi: 10.1109/IJCNN48605.2020.9206991.

[25] J. Heo, K. Song, S. Han, and D.-E. Lee, "Multi-channel convolutional neural network for integration of meteorological and geographical features in solar power forecasting," *Appl. Energy*, vol. 295, Aug. 2021, Art. no. 117083, doi: 10.1016/j.apenergy.2021.117083.

[26] N. Dong, J.-F. Chang, A.-G. Wu, and Z.-K. Gao, "A novel convolutional neural network framework based solar irradiance prediction method," *Int. J. Electr. Power Energy Syst.*, vol. 114, Jan. 2020, Art. no. 105411, doi: 10.1016/j.ijepes.2019.105411.

[27] K. Wang, X. Qi, and H. Liu, "A comparison of day-ahead photovoltaic power forecasting models based on deep learning neural network," *Appl. Energy*, vol. 251, Oct. 2019, Art. no. 113315, doi: 10.1016/j.apenergy.2019.113315.

[28] S. M. J. Jalali, S. Ahmadian, A. Kavousi-Fard, A. Khosravi, and S. Nahavandi, "Automated deep CNN-LSTM architecture design for solar irradiance forecasting," *IEEE Trans. Syst., Man, Cybern., Syst.*, vol. 52, no. 1, pp. 54–65, Jan. 2022, doi: 10.1109/TSMC.2021.3093519.

[29] A. H. Elsheikh, S. W. Sharshir, M. Abd Elaziz, A. E. Kabeel, W. Guilan, and Z. Haiou, "Modeling of solar energy systems using artificial neural network: A comprehensive review," *Sol. Energy*, vol. 180, pp. 622–639, Mar. 2019, doi: 10.1016/j.solener.2019.01.037.

[30] A. R. Pazikadin, D. Rifai, K. Ali, M. Z. Malik, A. N. Abdalla, and M. A. Faraj, "Solar irradiance measurement instrumentation and power solar generation forecasting based on artificial neural networks (ANN): A review of five years research trend," *Sci. Total Environ.*, vol. 715, May 2020, Art. no. 136848, doi: 10.1016/j.scitotenv.2020.136848.

[31] J. Antonanzas, N. Osorio, R. Escobar, R. Urraca, F. J. Martinez-de-Pison, and F. Antonanzas-Torres, "Review of photovoltaic power forecasting," *Sol. Energy*, vol. 136, pp. 78–111, Oct. 2016, doi: 10.1016/j.solener.2016.06.069.

[32] A. K. Yadav and S. S. Chandel, "Solar radiation prediction using artificial neural network techniques: A review," *Renew. Sustain. Energy Rev.*, vol. 33, pp. 772–781, May 2014, doi: 10.1016/j.rser.2013.08.055.

[33] G. Alkhayat and R. Mehmood, "A review and taxonomy of wind and solar energy forecasting methods based on deep learning," *Energy AI*, vol. 4, Jun. 2021, Art. no. 100060, doi: 10.1016/j.egyai.2021.100060.

[34] W.-C. Tsai, C.-S. Tu, C.-M. Hong, and W.-M. Lin, "A review of state-of-the-art and short-term forecasting models for solar PV power generation," *Energies*, vol. 16, no. 14, p. 5436, Jul. 2023, doi: 10.3390/en16145436.

[35] W. S. McCulloch and W. Pitts, "A logical calculus of the ideas immanent in nervous activity," *Bull. Math. Biophys.*, vol. 5, no. 4, pp. 115–133, Dec. 1943, doi: 10.1007/bf02478259.

[36] T. J. Sejnowski, "The unreasonable effectiveness of deep learning in artificial intelligence," *Proc. Nat. Acad. Sci. USA*, vol. 117, no. 48, pp. 30033–30038, Dec. 2020, doi: 10.1073/pnas.1907373117.

[37] R. C. Eberhart and R. W. Dobbins, "Early neural network development history: The age of Camelot," *IEEE Eng. Med. Biol. Mag.*, vol. 9, no. 3, pp. 15–18, Sep. 1990, doi: 10.1109/51.59207.

[38] T. J. Sejnowski, *The Deep Learning Revolution*. Cambridge, MA, USA: MIT Press, 2018.

[39] Y.-C. Wu and J.-W. Feng, "Development and application of artificial neural network," *Wireless Pers. Commun.*, vol. 102, no. 2, pp. 1645–1656, Sep. 2018, doi: 10.1007/s11277-017-5224-x.

[40] V. Lafargue, P. Garda, and E. Belhaire, "An analog implementation of the Boltzmann machine with programmable learning algorithms," in *VLSI for Neural Networks and Artificial Intelligence*, J. G. Delgado-Frias and W. R. Moore, Eds. Boston, MA, USA: Springer, 1994, pp. 45–52, doi: 10.1007/978-1-4899-1331-9_4.

[41] M. Bagherbeik, P. Ashtari, S. F. Mousavi, K. Kanda, H. Tamura, and A. Sheikholeslami, "A permutational Boltzmann machine with parallel tempering for solving combinatorial optimization problems," in *Parallel Problem Solving From Nature—PPSN XVI* (Lecture Notes in Computer Science), vol. 12269, T. Bäck, M. Preuss, A. Deutz, H. Wang, C. Doerr, M. Emmerich, and H. Trautmann, Eds. Cham, Switzerland: Springer, 2020, pp. 317–331, doi: 10.1007/978-3-030-58112-1_22.

[42] E. B. Baum, "On the capabilities of multilayer perceptrons," *J. Complex.*, vol. 4, no. 3, pp. 193–215, Sep. 1988, doi: 10.1016/0885-064x(88)90020-9.

[43] M. Nielsen, "How the backpropagation algorithm works," in *Neural Networks and Deep Learning*, ch. 2. Determination Press, Accessed: Dec. 26, 2019. [Online]. Available: http://neuralnetworksanddeeplearning.com/chap2.html

[44] S. Hochreiter and J. Schmidhuber, "Long short-term memory," *Neural Comput.*, vol. 9, no. 8, pp. 1735–1780, Nov. 1997, doi: 10.1162/neco.1997.9.8.1735.

[45] Y. Lecun, L. Bottou, Y. Bengio, and P. Haffner, "Gradient-based learning applied to document recognition," *Proc. IEEE*, vol. 86, no. 11, pp. 2278–2324, Nov. 1998, doi: 10.1109/5.726791.

[46] A. Graves and J. Schmidhuber, "Framewise phoneme classification with bidirectional LSTM and other neural network architectures," *Neural Netw.*, vol. 18, nos. 5–6, pp. 602–610, Jul. 2005, doi: 10.1016/j.neunet.2005.06.042.

[47] J. Chung, C. Gulcehre, K. Cho, and Y. Bengio, "Empirical evaluation of gated recurrent neural networks on sequence modeling," 2014, *arXiv:1412.3555*.

[48] K. He, X. Zhang, S. Ren, and J. Sun, "Deep residual learning for image recognition," 2015, *arXiv:1512.03385*.

[49] R. Rajamanickam and D. Baskaran, "Neural network model for biological waste management systems," in *Current Trends and Advances in Computer-Aided Intelligent Environmental Data Engineering*. Amsterdam, The Netherlands: Elsevier, 2022, pp. 393–415, doi: 10.1016/B978-0-323-85597-6.00010-0.

[50] A. Mahrouch and M. Ouassaid, "Primary frequency regulation based on deloaded control, ANN, and 3D-fuzzy logic controller for hybrid autonomous microgrid," *Technol. Econ. Smart Grids Sustain. Energy*, vol. 7, no. 1, p. 1, Jan. 2022, doi: 10.1007/s40866-022-00125-2.

[51] D. Patel, S. Patel, P. Patel, and M. Shah, "Solar radiation and solar energy estimation using ANN and fuzzy logic concept: A comprehensive and systematic study," *Environ. Sci. Pollut. Res.*, vol. 29, no. 22, pp. 32428–32442, May 2022, doi: 10.1007/s11356-022-19185-z.

[52] M. Uzair and N. Jamil, "Effects of hidden layers on the efficiency of neural networks," in *Proc. IEEE 23rd Int. Multitopic Conf. (INMIC)*, Bahawalpur, Pakistan, Nov. 2020, pp. 1–6, doi: 10.1109/INMIC50486.2020.9318195.

[53] D. Cannizzaro, A. Aliberti, L. Bottaccioli, E. Macii, A. Acquaviva, and E. Patti, "Solar radiation forecasting based on convolutional neural network and ensemble learning," *Expert Syst. Appl.*, vol. 181, Nov. 2021, Art. no. 115167, doi: 10.1016/j.eswa.2021.115167.

[54] S. Albawi, T. A. Mohammed, and S. Al-Zawi, "Understanding of a convolutional neural network," in *Proc. Int. Conf. Eng. Technol. (ICET)*, Antalya, Turkey, Aug. 2017, pp. 1–6, doi: 10.1109/ICEngTechnol.2017.8308186.

[55] P. Kumari and D. Toshniwal, "Deep learning models for solar irradiance forecasting: A comprehensive review," *J. Cleaner Prod.*, vol. 318, Oct. 2021, Art. no. 128566, doi: 10.1016/j.jclepro.2021.128566.

[56] M. Coskun, A. Uçar, Ö. Yildirim, and Y. Demir, "Face recognition based on convolutional neural network," in *Proc. Int. Conf. Modern Electr. Energy Syst. (MEES)*, Kremenchuk, Ukraine, Nov. 2017, pp. 376–379, doi: 10.1109/MEES.2017.8248937.

[57] H. Gholamalinejad and H. Khosravi, "Vehicle classification using a real-time convolutional structure based on DWT pooling layer and SE blocks," *Expert Syst. Appl.*, vol. 183, Nov. 2021, Art. no. 115420, doi: 10.1016/j.eswa.2021.115420.

[58] R. Yamashita, M. Nishio, R. K. G. Do, and K. Togashi, "Convolutional neural networks: An overview and application in radiology," *Insights into Imag.*, vol. 9, no. 4, pp. 611–629, Aug. 2018, doi: 10.1007/s13244-018-0639-9.

[59] C. Feng and J. Zhang, "SolarNet: A sky image-based deep convolutional neural network for intra-hour solar forecasting," *Sol. Energy*, vol. 204, pp. 71–78, Jul. 2020, doi: 10.1016/j.solener.2020.03.083.

[60] I. Sutskever, J. Martens, and G. E. Hinton, "Generating text with recurrent neural networks," in *Proc. 28th Int. Conf. Mach. Learn.*, 2011, pp. 1017–1024. [Online]. Available: https://dl.acm.org/doi/10.5555/3104482.3104610

[61] A. Graves, "Generating sequences with recurrent neural networks," 2013, *arXiv:1308.0850*.

[62] H. Salehinejad, S. Sankar, J. Barfett, E. Colak, and S. Valaee, "Recent advances in recurrent neural networks," 2018, *arXiv:1801.01078*.

[63] S.-C. Lim, J.-H. Huh, S.-H. Hong, C.-Y. Park, and J.-C. Kim, "Solar power forecasting using CNN-LSTM hybrid model," *Energies*, vol. 15, no. 21, p. 8233, Nov. 2022, doi: 10.3390/en15218233.

[64] T. Mikolov, A. Joulin, S. Chopra, M. Mathieu, and M. Ranzato, "Learning longer memory in recurrent neural networks," 2014, *arXiv:1412.7753*.

[65] C. Olah. (2015). *Understanding LSTM Networks*. Accessed: Aug. 27, 2015. [Online]. Available: https://colah.github.io/posts/2015-08-Understanding-LSTMs/

[66] G. Kumar, U. P. Singh, and S. Jain, "An adaptive particle swarm optimization-based hybrid long short-term memory model for stock price time series forecasting," *Soft Comput.*, vol. 26, no. 22, pp. 12115–12135, Nov. 2022, doi: 10.1007/s00500-022-07451-8.

[67] K. Cho, B. van Merrienboer, C. Gulcehre, D. Bahdanau, F. Bougares, H. Schwenk, and Y. Bengio, "Learning phrase representations using RNN encoder–decoder for statistical machine translation," 2014, *arXiv:1406.1078*.

[68] K. Park, Y. Seong, Y. Jung, I. Youn, and C. K. Choi, "Development of water level prediction improvement method using multivariate time series data by GRU model," *Water*, vol. 15, no. 3, p. 587, Feb. 2023, doi: 10.3390/w15030587.

[69] J. Zhang, A. Florita, B.-M. Hodge, S. Lu, H. F. Hamann, V. Banunarayanan, and A. M. Brockway, "A suite of metrics for assessing the performance of solar power forecasting," *Sol. Energy*, vol. 111, pp. 157–175, Jan. 2015, doi: 10.1016/j.solener.2014.10.016.

[70] B. Uzum, A. Onen, H. M. Hasanien, and S. M. Muyeen, "Rooftop solar PV penetration impacts on distribution network and further growth factors—A comprehensive review," *Electronics*, vol. 10, no. 1, p. 55, Dec. 2020, doi: 10.3390/electronics10010055.

[71] B. Kraas, M. Schroedter-Homscheidt, and R. Madlener, ''Economic merits of a state-of-the-art concentrating solar power forecasting system for participation in the Spanish electricity market,'' *Sol. Energy*, vol. 93, pp. 244–255, Jul. 2013, doi: 10.1016/j.solener.2013.04.012.

[72] Y. Wang, D. Millstein, A. D. Mills, S. Jeong, and A. Ancell, ''The cost of day-ahead solar forecasting errors in the united states,'' *Sol. Energy*, vol. 231, pp. 846–856, Jan. 2022, doi: 10.1016/j.solener.2021.12.012.

[73] X.-H. Le, H. V. Ho, G. Lee, and S. Jung, ''Application of long short-term memory (LSTM) neural network for flood forecasting,'' *Water*, vol. 11, no. 7, p. 1387, Jul. 2019, doi: 10.3390/w11071387.

[74] V. Bui, N. T. Le, V. H. Nguyen, J. Kim, and Y. M. Jang, ''Multi-behavior with bottleneck features LSTM for load forecasting in building energy management system,'' *Electronics*, vol. 10, no. 9, p. 1026, Apr. 2021, doi: 10.3390/electronics10091026.

[75] B. H. Vu and I.-Y. Chung, ''Optimal generation scheduling and operating reserve management for PV generation using RNN-based forecasting models for stand-alone microgrids,'' *Renew. Energy*, vol. 195, pp. 1137–1154, Aug. 2022, doi: 10.1016/j.renene.2022.06.086.

[76] F. Golestaneh, P. Pinson, and H. B. Gooi, ''Very short-term nonparametric probabilistic forecasting of renewable energy generation—With application to solar energy,'' *IEEE Trans. Power Syst.*, vol. 31, no. 5, pp. 3850–3863, Sep. 2016, doi: 10.1109/TPWRS.2015.2502423.

[77] F. Barbieri, S. Rajakaruna, and A. Ghosh, ''Very short-term photovoltaic power forecasting with cloud modeling: A review,'' *Renew. Sustain. Energy Rev.*, vol. 75, pp. 242–263, Aug. 2017, doi: 10.1016/j.rser.2016.10.068.

[78] M. Rana, I. Koprinska, and V. G. Agelidis, ''Univariate and multivariate methods for very short-term solar photovoltaic power forecasting,'' *Energy Convers. Manage.*, vol. 121, pp. 380–390, Aug. 2016, doi: 10.1016/j.enconman.2016.05.025.

[79] H. Panamtash, S. Mahdavi, Q. Z. Sun, G.-J. Qi, H. Liu, and A. Dimitrovski, ''Very short-term solar power forecasting using a frequency incorporated deep learning model,'' *IEEE Open Access J. Power Energy*, vol. 10, pp. 517–527, 2023, doi: 10.1109/OAJPE.2023.3294457.

[80] A. Rafati, M. Joorabian, E. Mashhour, and H. R. Shaker, ''High dimensional very short-term solar power forecasting based on a data-driven heuristic method,'' *Energy*, vol. 219, Mar. 2021, Art. no. 119647, doi: 10.1016/j.energy.2020.119647.

[81] H. Panamtash, R. York, P. Brooker, J. Kramer, and Q. Z. Sun, ''Solar power smoothing in a nanogrid testbed,'' 2022, *arXiv:2206.15323*.

[82] F. P. M. Kreuwel, W. H. Knap, L. R. Visser, W. G. J. H. M. van Sark, J. V.-G. de Arellano, and C. C. van Heerwaarden, ''Analysis of high frequency photovoltaic solar energy fluctuations,'' *Sol. Energy*, vol. 206, pp. 381–389, Aug. 2020, doi: 10.1016/j.solener.2020.05.093.

[83] R. Asghar, M. H. Sulaiman, S. Saeed, H. Wadood, T. K. Mehmand, and Z. Ullah, ''Application of linear and nonlinear control schemes for the stability of smart grid,'' in *Proc. Int. Conf. Emerg. Technol. Electron., Comput. Commun. (ICETECC)*, Jamshoro, Pakistan, Dec. 2022, pp. 1–6, doi: 10.1109/ICETECC56662.2022.10069570.

[84] A. M. Assaf, H. Haron, H. N. A. Hamed, F. A. Ghaleb, S. N. Qasem, and A. M. Albarrak, ''A review on neural network based models for short term solar irradiance forecasting,'' *Appl. Sci.*, vol. 13, no. 14, p. 8332, Jul. 2023, doi: 10.3390/app13148332.

[85] International Renewable Energy Agency, Abu Dhabi, United Arab Emirates. (2020). *Advanced Forecasting of Variable Renewable Power Generation*. [Online]. Available: https://www.irena.org/-/media/Files/IRENA/Agency/Publication/2020/Jul/IRENA_Advanced_weather_forecasting_2020.pdf

[86] Y. Ren, P. N. Suganthan, and N. Srikanth, ''Ensemble methods for wind and solar power forecasting—A state-of-the-art review,'' *Renew. Sustain. Energy Rev.*, vol. 50, pp. 82–91, Oct. 2015, doi: 10.1016/j.rser.2015.04.081.

[87] D. J. Pedregal and J. R. Trapero, ''Adjusted combination of moving averages: A forecasting system for medium-term solar irradiance,'' *Appl. Energy*, vol. 298, Sep. 2021, Art. no. 117155, doi: 10.1016/j.apenergy.2021.117155.

[88] E. Doddy Clarke and C. Sweeney, ''Solar energy and weather,'' *Weather*, vol. 77, no. 3, pp. 90–91, Mar. 2022, doi: 10.1002/wea.4124.

[89] Y.-J. Zhong and Y.-K. Wu, ''Short-term solar power forecasts considering various weather variables,'' in *Proc. Int. Symp. Comput., Consum. Control (IS3C)*, Taiwan, Nov. 2020, pp. 432–435, doi: 10.1109/IS3C50286.2020.00117.

[90] M. Tahri, M. Hakdaoui, and M. Maanan, ''The evaluation of solar farm locations applying geographic information system and multi-criteria decision-making methods: Case study in Morocco,'' *Renew. Sustain. Energy Rev.*, vol. 51, pp. 1354–1362, Nov. 2015, doi: 10.1016/j.rser.2015.07.054.

[91] H. Zhu, X. Li, Q. Sun, L. Nie, J. Yao, and G. Zhao, ''A power prediction method for photovoltaic power plant based on wavelet decomposition and artificial neural networks,'' *Energies*, vol. 9, no. 1, p. 11, Dec. 2015, doi: 10.3390/en9010011.

[92] N. Son and M. Jung, ''Analysis of meteorological factor multivariate models for medium- and long-term photovoltaic solar power forecasting using long short-term memory,'' *Appl. Sci.*, vol. 11, no. 1, p. 316, Dec. 2020, doi: 10.3390/app11010316.

[93] P. A. G. M. Amarasinghe, N. S. Abeygunawardana, T. N. Jayasekara, E. A. J. P. Edirisinghe, and S. K. Abeygunawardane, ''Ensemble models for solar power forecasting—A weather classification approach,'' *AIMS Energy*, vol. 8, no. 2, pp. 252–271, 2020, doi: 10.3934/energy.2020.2.252.

[94] B. Carrera, M. Sim, and J. Jung, ''PVHybNet: A hybrid framework for predicting photovoltaic power generation using both weather forecast and observation data,'' *IET Renew. Power Gener.*, vol. 14, no. 12, pp. 2192–2201, Sep. 2020, doi: 10.1049/iet-rpg.2018.6174.

[95] H. Sangrody, M. Sarailoo, N. Zhou, N. Tran, M. Motalleb, and E. Foruzan, ''Weather forecasting error in solar energy forecasting,'' *IET Renew. Power Gener.*, vol. 11, no. 10, pp. 1274–1280, Aug. 2017, doi: 10.1049/iet-rpg.2016.1043.

[96] S. Lamp, ''Sunspots that matter: The effect of weather on solar technology adoption,'' *Environ. Resource Econ.*, vol. 84, no. 4, pp. 1179–1219, Apr. 2023, doi: 10.1007/s10640-022-00753-3.

[97] H. G. Beyer, J. P. Martinez, M. Suri, J. L. Torres, E. Lorenz, S. C. Müller, C. Hoyer-Klick, and P. Ineichen. (2009). *Report on Benchmarking of Radiation Products*. Accessed: Aug. 27, 2009. [Online]. Available: https://www.researchgate.net/publication/265362324_Report_on_Benchmarking_of_Radiation_Products

[98] H. J. Payne, S. Hemming, B. A. P. van Rens, E. J. van Henten, and S. van Mourik, ''Quantifying the role of weather forecast error on the uncertainty of greenhouse energy prediction and power market trading,'' *Biosystems Eng.*, vol. 224, pp. 1–15, Dec. 2022, doi: 10.1016/j.biosystemseng.2022.09.009.

[99] D. Orrell, L. Smith, J. Barkmeijer, and T. N. Palmer, ''Model error in weather forecasting,'' *Nonlinear Processes Geophys.*, vol. 8, no. 6, pp. 357–371, Dec. 2001.

[100] V. Plevris, G. Solorzano, N. Bakas, and M. B. Seghier, ''Investigation of performance metrics in regression analysis and machine learning-based prediction models,'' in *Proc. 8th Eur. Congr. Comput. Methods Appl. Sci. Eng.*, 2022, pp. 1–25, doi: 10.23967/eccomas.2022.155.

[101] O. I. Abiodun, A. Jantan, A. E. Omolara, K. V. Dada, N. A. Mohamed, and H. Arshad, ''State-of-the-art in artificial neural network applications: A survey,'' *Heliyon*, vol. 4, no. 11, Nov. 2018, Art. no. e00938, doi: 10.1016/j.heliyon.2018.e00938.

[102] S. Makridakis, E. Spiliotis, and V. Assimakopoulos, ''Statistical and machine learning forecasting methods: Concerns and ways forward,'' *PLoS ONE*, vol. 13, no. 3, Mar. 2018, Art. no. e0194889, doi: 10.1371/journal.pone.0194889.

[103] A. Botchkarev, ''A new typology design of performance metrics to measure errors in machine learning regression algorithms,'' *Interdiscipl. J. Inf., Knowl., Manage.*, vol. 14, pp. 45–76, Jan. 2019, doi: 10.28945/4184.

[104] M. Hossin and M. N. Sulaiman, ''A review on evaluation metrics for data classification evaluations,'' *Int. J. Data Mining Knowl. Manage. Process*, vol. 5, no. 2, pp. 1–11, Mar. 2015, doi: 10.5121/ijdkp.2015.5201.

[105] R. Caruana and A. Niculescu-Mizil, ''Data mining in metric space: An empirical analysis of supervised learning performance criteria,'' in *Proc. 10th ACM SIGKDD Int. Conf. Knowl. Discovery Data Mining*. Seattle, WA, USA, Aug. 2004, pp. 69–78, doi: 10.1145/1014052.1014063.

[106] J. Zhu, Z. Zhao, X. Zheng, Z. An, Q. Guo, Z. Li, J. Sun, and Y. Guo, ''Time-series power forecasting for wind and solar energy based on the SL-transformer,'' *Energies*, vol. 16, no. 22, p. 7610, Nov. 2023, doi: 10.3390/en16227610.

[107] Y. Ledmaoui, A. El Maghraoui, M. El Aroussi, R. Saadane, A. Chebak, and A. Chehri, ''Forecasting solar energy production: A comparative study of machine learning algorithms,'' *Energy Rep.*, vol. 10, pp. 1004–1012, Nov. 2023, doi: 10.1016/j.egyr.2023.07.042.

[108] L. Gutiérrez, J. Patiño, and E. Duque-Grisales, ''A comparison of the performance of supervised learning algorithms for solar power prediction,'' *Energies*, vol. 14, no. 15, p. 4424, Jul. 2021, doi: 10.3390/en14154424.

[109] A. M. Kuriakose, D. P. Kariyalil, M. Augusthy, S. Sarath, J. Jacob, and N. R. Antony, "Comparison of artificial neural network, linear regression and support vector machine for prediction of solar PV power," in *Proc. IEEE Pune Sect. Int. Conf. (PuneCon)*, Pune, India, Dec. 2020, pp. 1–6, doi: 10.1109/PuneCon50868.2020.9362442.

[110] A. Alcañiz, D. Grzebyk, H. Ziar, and O. Isabella, "Trends and gaps in photovoltaic power forecasting with machine learning," *Energy Rep.*, vol. 9, pp. 447–471, Dec. 2023, doi: 10.1016/j.egyr.2022.11.208.

[111] M. N. Akhter, S. Mekhilef, H. Mokhlis, R. Ali, M. Usama, M. A. Muhammad, and A. S. M. Khairuddin, "A hybrid deep learning method for an hour ahead power output forecasting of three different photovoltaic systems," *Appl. Energy*, vol. 307, Feb. 2022, Art. no. 118185, doi: 10.1016/j.apenergy.2021.118185.

[112] V. Lucaferri, M. Quercio, A. Laudani, and F. R. Fulginei, "A review on battery model-based and data-driven methods for battery management systems," *Energies*, vol. 16, no. 23, p. 7807, Nov. 2023, doi: 10.3390/en16237807.

[113] G. Graditi, S. Ferlito, and G. Adinolfi, "Comparison of photovoltaic plant power production prediction methods using a large measured dataset," *Renew. Energy*, vol. 90, pp. 513–519, May 2016, doi: 10.1016/j.renene.2016.01.027.

[114] G. M. Lozito, L. Bozzoli, and A. Salvini, "Microcontroller based maximum power point tracking through FCC and MLP neural networks," in *Proc. 6th Eur. Embedded Design Educ. Res. Conf. (EDERC)*, Milano, Italy, Sep. 2014, pp. 207–211, doi: 10.1109/EDERC.2014.6924389.

[115] D. A. Fadare, "Modelling of solar energy potential in Nigeria using an artificial neural network model," *Appl. Energy*, vol. 86, no. 9, pp. 1410–1422, Sep. 2009, doi: 10.1016/j.apenergy.2008.12.005.

[116] F. Rodríguez, M. Genn, L. Fontán, and A. Galarza, "Very short-term temperature forecaster using MLP and N-nearest stations for calculating key control parameters in solar photovoltaic generation," *Sustain. Energy Technol. Assessments*, vol. 45, Jun. 2021, Art. no. 101085, doi: 10.1016/j.seta.2021.101085.

[117] A. F. Mashaly and A. A. Alazba, "MLP and MLR models for instantaneous thermal efficiency prediction of solar still under hyper-arid environment," *Comput. Electron. Agricult.*, vol. 122, pp. 146–155, Mar. 2016, doi: 10.1016/j.compag.2016.01.030.

[118] J. H. Yousif and H. A. Kazem, "Modeling of daily solar energy system prediction using soft computing methods for Oman," *Res. J. Appl. Sci., Eng. Technol.*, vol. 13, no. 3, pp. 237–244, Aug. 2016, doi: 10.19026/rjaset.13.2936.

[119] Y. Yu, J. Cao, and J. Zhu, "An LSTM short-term solar irradiance forecasting under complicated weather conditions," *IEEE Access*, vol. 7, pp. 145651–145666, 2019, doi: 10.1109/ACCESS.2019.2946057.

[120] Y. Yu, J. Cao, X. Wan, F. Zeng, J. Xin, and Q. Ji, "Comparison of short-term solar irradiance forecasting methods when weather conditions are complicated," *J. Renew. Sustain. Energy*, vol. 10, no. 5, Sep. 2018, Art. no. 053501, doi: 10.1063/1.5041905.

[121] R. Sivanand, J. Singh, A. Ali, A. Khan, and M. F. Hoda, "A comparative study of different deep learning models for mid-term solar power prediction," in *Proc. Int. Conf. Advance Comput. Innov. Technol. Eng. (ICACITE)*, Greater Noida, India, Mar. 2021, pp. 519–524, doi: 10.1109/ICACITE51222.2021.9404630.

[122] S. Boubaker, M. Benghanem, A. Mellit, A. Lefza, O. Kahouli, and L. Kolsi, "Deep neural networks for predicting solar radiation at Hail region, Saudi Arabia," *IEEE Access*, vol. 9, pp. 36719–36729, 2021, doi: 10.1109/ACCESS.2021.3062205.

[123] J. Wojtkiewicz, M. Hosseini, R. Gottumukkala, and T. L. Chambers, "Hour-ahead solar irradiance forecasting using multivariate gated recurrent units," *Energies*, vol. 12, no. 21, p. 4055, Oct. 2019, doi: 10.3390/en12214055.

[124] A. Zameer, F. Jaffar, F. Shahid, M. Muneeb, R. Khan, and R. Nasir, "Short-term solar energy forecasting: Integrated computational intelligence of LSTMs and GRU," *PLoS ONE*, vol. 18, no. 10, Oct. 2023, Art. no. e0285410, doi: 10.1371/journal.pone.0285410.

[125] K. Wang, X. Qi, and H. Liu, "Photovoltaic power forecasting based LSTM-convolutional network," *Energy*, vol. 189, Dec. 2019, Art. no. 116225, doi: 10.1016/j.energy.2019.116225.

[126] Z. Song and L. E. Brown, "Multi-dimensional evaluation of temporal neural networks on solar irradiance forecasting," in *Proc. IEEE Innov. Smart Grid Technol. Asia (ISGT Asia)*, Chengdu, China, May 2019, pp. 4192–4197, doi: 10.1109/ISGT-Asia.2019.8881784.

[127] J. Jeong and H. Kim, "Multi-site photovoltaic forecasting exploiting space-time convolutional neural network," *Energies*, vol. 12, no. 23, p. 4490, Nov. 2019, doi: 10.3390/en12234490.

[128] H. Zang, L. Cheng, T. Ding, K. W. Cheung, Z. Wei, and G. Sun, "Day-ahead photovoltaic power forecasting approach based on deep convolutional neural networks and meta learning," *Int. J. Electr. Power Energy Syst.*, vol. 118, Jun. 2020, Art. no. 105790, doi: 10.1016/j.ijepes.2019.105790.

[129] D. Lee, J. Jeong, S. H. Yoon, and Y. T. Chae, "Improvement of short-term BIPV power predictions using feature engineering and a recurrent neural network," *Energies*, vol. 12, no. 17, p. 3247, Aug. 2019, doi: 10.3390/en12173247.

[130] C. Huang, L. Cao, N. Peng, S. Li, J. Zhang, L. Wang, X. Luo, and J.-H. Wang, "Day-ahead forecasting of hourly photovoltaic power based on robust multilayer perception," *Sustainability*, vol. 10, no. 12, p. 4863, Dec. 2018, doi: 10.3390/su10124863.

[131] A. Golder, J. Jneid, J. Zhao, and F. Bouffard, "Machine learning-based demand and PV power forecasts," in *Proc. IEEE Electr. Power Energy Conf. (EPEC)*, Montreal, QC, Canada, Oct. 2019, pp. 1–6, doi: 10.1109/EPEC47565.2019.9074819.

[132] N. Q. Nguyen, L. D. Bui, B. V. Doan, E. R. Sanseverino, D. D. Cara, and Q. D. Nguyen, "A new method for forecasting energy output of a large-scale solar power plant based on long short-term memory networks a case study in Vietnam," *Electr. Power Syst. Res.*, vol. 199, Oct. 2021, Art. no. 107427, doi: 10.1016/j.epsr.2021.107427.

[133] G. Li, H. Wang, S. Zhang, J. Xin, and H. Liu, "Recurrent neural networks based photovoltaic power forecasting approach," *Energies*, vol. 12, no. 13, p. 2538, Jul. 2019, doi: 10.3390/en12132538.

[134] A. Mellit, A. M. Pavan, and V. Lughi, "Deep learning neural networks for short-term photovoltaic power forecasting," *Renew. Energy*, vol. 172, pp. 276–288, Jul. 2021, doi: 10.1016/j.renene.2021.02.166.

[135] M. S. Hossain and H. Mahmood, "Short-term photovoltaic power forecasting using an LSTM neural network and synthetic weather forecast," *IEEE Access*, vol. 8, pp. 172524–172533, 2020, doi: 10.1109/ACCESS.2020.3024901.

[136] J. Zhang, R. Verschae, S. Nobuhara, and J.-F. Lalonde, "Deep photovoltaic nowcasting," *Sol. Energy*, vol. 176, pp. 267–276, Dec. 2018, doi: 10.1016/j.solener.2018.10.024.

[137] T. Limouni, R. Yaagoubi, K. Bouziane, K. Guissi, and E. H. Baali, "Univariate and multivariate LSTM models for one step and multistep PV power forecasting," *Int. J. Renew. Energy Develop.*, vol. 11, no. 3, pp. 815–828, Aug. 2022, doi: 10.14710/ijred.2022.43953.

[138] W.-C. Kuo, C.-H. Chen, S.-Y. Chen, and C.-C. Wang, "Deep learning neural networks for short-term PV power forecasting via sky image method," *Energies*, vol. 15, no. 13, p. 4779, Jun. 2022, doi: 10.3390/en15134779.

[139] W.-C. Kuo, C.-H. Chen, S.-H. Hua, and C.-C. Wang, "Assessment of different deep learning methods of power generation forecasting for solar PV system," *Appl. Sci.*, vol. 12, no. 15, p. 7529, Jul. 2022, doi: 10.3390/app12157529.

[140] A.-N. Buturache and S. Stancu, "Solar energy production forecast using standard recurrent neural networks, long short-term memory, and gated recurrent unit," *Eng. Econ.*, vol. 32, no. 4, pp. 313–324, Oct. 2021, doi: 10.5755/j01.ee.32.4.28459.

[141] S. Thejus and P. Sivraj, "Deep learning-based power consumption and generation forecasting for demand side management," in *Proc. 2nd Int. Conf. Electron. Sustain. Commun. Syst. (ICESC)*, Coimbatore, India, Aug. 2021, pp. 1350–1357, doi: 10.1109/ICESC51422.2021.9532707.

[142] S. Khan, F. Shaikh, M. M. Siddiqui, T. Hussain, L. Kumar, and A. Nahar, "Hourly forecasting of solar photovoltaic power in Pakistan using recurrent neural networks," *Int. J. Photoenergy*, vol. 2022, pp. 1–11, Jan. 2022, doi: 10.1155/2022/7015818.

[143] L. Yunqiao and F. Yan, "An innovative power prediction method for bifacial PV modules," *Electr. Eng.*, vol. 105, no. 4, pp. 2151–2159, Aug. 2023, doi: 10.1007/s00202-023-01805-7.

[144] L. Du, L. Zhang, and X. Tian, "Deep power forecasting model for building attached photovoltaic system," *IEEE Access*, vol. 6, pp. 52639–52651, 2018, doi: 10.1109/ACCESS.2018.2869424.

[145] C.-J. Huang and P.-H. Kuo, "Multiple-input deep convolutional neural network model for short-term photovoltaic power forecasting," *IEEE Access*, vol. 7, pp. 74822–74834, 2019, doi: 10.1109/ACCESS.2019.2921238.

[146] M. Massaoudi, I. Chihi, L. Sidhom, M. Trabelsi, S. S. Refaat, and F. S. Oueslati, ''Performance evaluation of deep recurrent neural networks architectures: Application to PV power forecasting,'' in *Proc. 2nd Int. Conf. Smart Grid Renew. Energy (SGRE)*, Doha, Qatar, Nov. 2019, pp. 1–6, doi: 10.1109/SGRE46976.2019.9020965.

[147] F. R. Fulginei, A. Salvini, and G. Pulcini, ''Metric-topological–evolutionary optimization,'' *Inverse Problems Sci. Eng.*, vol. 20, no. 1, pp. 41–58, Jan. 2012, doi: 10.1080/17415977.2011.624624.

[148] M. Neshat, M. M. Nezhad, S. Mirjalili, D. A. Garcia, E. Dahlquist, and A. H. Gandomi, ''Short-term solar radiation forecasting using hybrid deep residual learning and gated LSTM recurrent network with differential covariance matrix adaptation evolution strategy,'' *Energy*, vol. 278, Sep. 2023, Art. no. 127701, doi: 10.1016/j.energy.2023.127701.

[149] A. Kumar, M. Rizwan, and U. Nangia, ''A hybrid intelligent approach for solar photovoltaic power forecasting: Impact of aerosol data,'' *Arabian J. Sci. Eng.*, vol. 45, no. 3, pp. 1715–1732, Mar. 2020, doi: 10.1007/s13369-019-04183-0.

[150] M. Colak, M. Yesilbudak, and R. Bayindir, ''Daily photovoltaic power prediction enhanced by hybrid GWO-MLP, ALO-MLP and WOA-MLP models using meteorological information,'' *Energies*, vol. 13, no. 4, p. 901, Feb. 2020, doi: 10.3390/en13040901.

[151] T. Vaisakh and R. Jayabarathi, ''Analysis on intelligent machine learning enabled with meta-heuristic algorithms for solar irradiance prediction,'' *Evol. Intell.*, vol. 15, no. 1, pp. 235–254, Mar. 2022, doi: 10.1007/s12065-020-00505-6.

[152] W. Bendali, I. Saber, B. Bourachdi, M. Boussetta, and Y. Mourad, ''Deep learning using genetic algorithm optimization for short term solar irradiance forecasting,'' in *Proc. 4th Int. Conf. Intell. Comput. Data Sci. (ICDS)*, Fez, Morocco, Oct. 2020, pp. 1–8, doi: 10.1109/ICDS50568.2020.9268682.

[153] S. Jaidee and W. Pora, ''Very short-term solar power forecasting using genetic algorithm based deep neural network,'' in *Proc. 4th Int. Conf. Inf. Technol. (InCIT)*, Bangkok, Thailand, Oct. 2019, pp. 184–189, doi: 10.1109/INCIT.2019.8912097.

[154] T. Zhu, Y. Li, Z. Li, Y. Guo, and C. Ni, ''Inter-hour forecast of solar radiation based on long short-term memory with attention mechanism and genetic algorithm,'' *Energies*, vol. 15, no. 3, p. 1062, Jan. 2022, doi: 10.3390/en15031062.

[155] Z. Huang, J. Huang, and J. Min, ''SSA-LSTM: Short-term photovoltaic power prediction based on feature matching,'' *Energies*, vol. 15, no. 20, p. 7806, Oct. 2022, doi: 10.3390/en15207806.

[156] A. A. Ewees, M. A. A. Al-Qaness, L. Abualigah, and M. A. Elaziz, ''HBO-LSTM: Optimized long short term memory with heap-based optimizer for wind power forecasting,'' *Energy Convers. Manage.*, vol. 268, Sep. 2022, Art. no. 116022, doi: 10.1016/j.enconman.2022.116022.

[157] C. Stoean, M. Zivkovic, A. Bozovic, N. Bacanin, R. Strulak-Wójcikiewicz, M. Antonijevic, and R. Stoean, ''Metaheuristic-based hyperparameter tuning for recurrent deep learning: Application to the prediction of solar energy generation,'' *Axioms*, vol. 12, no. 3, p. 266, Mar. 2023, doi: 10.3390/axioms12030266.

[158] N. Bacanin, L. Jovanovic, M. Zivkovic, V. Kandasamy, M. Antonijevic, M. Deveci, and I. Strumberger, ''Multivariate energy forecasting via metaheuristic tuned long-short term memory and gated recurrent unit neural networks,'' *Inf. Sci.*, vol. 642, Sep. 2023, Art. no. 119122, doi: 10.1016/j.ins.2023.119122.

[159] H. Ma, C. Zhang, T. Peng, M. S. Nazir, and Y. Li, ''An integrated framework of gated recurrent unit based on improved sine cosine algorithm for photovoltaic power forecasting,'' *Energy*, vol. 256, Oct. 2022, Art. no. 124650, doi: 10.1016/j.energy.2022.124650.

[160] H. Aprillia, H.-T. Yang, and C.-M. Huang, ''Short-term photovoltaic power forecasting using a convolutional neural network–salp swarm algorithm,'' *Energies*, vol. 13, no. 8, p. 1879, Apr. 2020, doi: 10.3390/en13081879.

[161] J. Liu, Q. Shi, R. Han, and J. Yang, ''A hybrid GA–PSO–CNN model for ultra-short-term wind power forecasting,'' *Energies*, vol. 14, no. 20, p. 6500, Oct. 2021, doi: 10.3390/en14206500.

[162] H. Zhou, Q. Liu, K. Yan, and Y. Du, ''Deep learning enhanced solar energy forecasting with AI-driven IoT,'' *Wireless Commun. Mobile Comput.*, vol. 2021, pp. 1–11, Jun. 2021, doi: 10.1155/2021/9249387.

[163] L. D. Soares and E. M. C. Franco, ''BiGRU-CNN neural network applied to short-term electric load forecasting,'' *Production*, vol. 32, Dec. 2022, Art. no. e20210087, doi: 10.1590/0103-6513.20210087.

[164] Y. Dai, Y. Wang, M. Leng, X. Yang, and Q. Zhou, ''Short-term photovoltaic power generation forecasting with lowess smoothing, feature selection, and optimized BiGRU,'' *SSRN*, pp. 1–26, Mar. 2023, doi: 10.2139/ssrn.4374906.

[165] X. Huang, Q. Li, Y. Tai, Z. Chen, J. Zhang, J. Shi, B. Gao, and W. Liu, ''Hybrid deep neural model for hourly solar irradiance forecasting,'' *Renew. Energy*, vol. 171, pp. 1041–1060, Jun. 2021, doi: 10.1016/j.renene.2021.02.161.

[166] N. P. Sebi, ''Intelligent solar irradiance forecasting using hybrid deep learning model: A Meta-Heuristic-Based prediction,'' *Neural Process. Lett.*, vol. 55, no. 2, pp. 1247–1280, Apr. 2023, doi: 10.1007/s11063-022-10935-1.

[167] H. T. C. Pedro and C. F. M. Coimbra, ''Assessment of forecasting techniques for solar power production with no exogenous inputs,'' *Sol. Energy*, vol. 86, no. 7, pp. 2017–2028, Jul. 2012, doi: 10.1016/j.solener.2012.04.004.

[168] J. Zheng, H. Zhang, Y. Dai, B. Wang, T. Zheng, Q. Liao, Y. Liang, F. Zhang, and X. Song, ''Time series prediction for output of multi-region solar power plants,'' *Appl. Energy*, vol. 257, Jan. 2020, Art. no. 114001, doi: 10.1016/j.apenergy.2019.114001.

[169] S. Wang, L. Zhou, and H. Fu, ''Short-term photovoltaic power prediction based on ICHOA-GRU,'' in *Proc. 5th Int. Conf. Intell. Control, Meas. Signal Process. (ICMSP)*, Chengdu, China, May 2023, pp. 1–8, doi: 10.1109/ICMSP58539.2023.10171058.

[170] H. Zhen, D. Niu, K. Wang, Y. Shi, Z. Ji, and X. Xu, ''Photovoltaic power forecasting based on GA improved bi-LSTM in microgrid without meteorological information,'' *Energy*, vol. 231, Sep. 2021, Art. no. 120908, doi: 10.1016/j.energy.2021.120908.

[171] M. Tovar, M. Robles, and F. Rashid, ''PV power prediction, using CNN-LSTM hybrid neural network model. Case of study: Temixco–Morelos, México,'' *Energies*, vol. 13, no. 24, p. 6512, Dec. 2020, doi: 10.3390/en13246512.

[172] A. Rai, A. Shrivastava, and K. C. Jana, ''A robust auto encoder-gated recurrent unit (AE-GRU) based deep learning approach for short term solar power forecasting,'' *Optik*, vol. 252, Feb. 2022, Art. no. 168515, doi: 10.1016/j.ijleo.2021.168515.

[173] H. Alharkan, S. Habib, and M. Islam, ''Solar power prediction using dual stream CNN-LSTM architecture,'' *Sensors*, vol. 23, no. 2, p. 945, Jan. 2023, doi: 10.3390/s23020945.

[174] A. Rai, A. Shrivastava, and K. C. Jana, ''Differential attention net: Multi-directed differential attention based hybrid deep learning model for solar power forecasting,'' *Energy*, vol. 263, Jan. 2023, Art. no. 125746, doi: 10.1016/j.energy.2022.125746.

[175] M. Khan, M. Ishaq, and S. Kwon, ''A CNN-assisted deep echo state network using multiple time-scale dynamic learning reservoirs for generating short-term solar energy forecasting,'' *Sustain. Energy Technol. Assessments*, vol. 52, Aug. 2022, Art. no. 102275, doi: 10.1016/j.seta.2022.102275.

[176] M. Sabri and M. El Hassouni, ''Predicting photovoltaic power generation using double-layer bidirectional long short-term memory-convolutional network,'' *Int. J. Energy Environ. Eng.*, vol. 14, no. 3, pp. 497–510, Sep. 2023, doi: 10.1007/s40095-022-00530-4.

[177] C. Zhang, T. Peng, and M. S. Nazir, ''A novel integrated photovoltaic power forecasting model based on variational mode decomposition and CNN-BiGRU considering meteorological variables,'' *Electr. Power Syst. Res.*, vol. 213, Dec. 2022, Art. no. 108796, doi: 10.1016/j.epsr.2022.108796.

[178] A. F. Mirza, M. Mansoor, M. Usman, and Q. Ling, ''A comprehensive approach for PV wind forecasting by using a hyperparameter tuned GCVCNN-MRNN deep learning model,'' *Energy*, vol. 283, Nov. 2023, Art. no. 129189, doi: 10.1016/j.energy.2023.129189.

[179] M. A. Houran, S. M. S. Bukhari, M. H. Zafar, M. Mansoor, and W. Chen, ''COA-CNN-LSTM: Coati optimization algorithm-based hybrid deep learning model for PV/wind power forecasting in smart grid applications,'' *Appl. Energy*, vol. 349, Nov. 2023, Art. no. 121638, doi: 10.1016/j.apenergy.2023.121638.

[180] S. Yang, X. Yu, and Y. Zhou, ''LSTM and GRU neural network performance comparison study: Taking yelp review dataset as an example,'' in *Proc. Int. Workshop Electron. Commun. Artif. Intell. (IWECAI)*, Shanghai, China, Jun. 2020, pp. 98–101, doi: 10.1109/IWECAI50956.2020.00027.

[181] R. A. Rajagukguk, R. A. A. Ramadhan, and H.-J. Lee, "A review on deep learning models for forecasting time series data of solar irradiance and photovoltaic power," *Energies*, vol. 13, no. 24, p. 6623, Dec. 2020, doi: 10.3390/en13246623.

[182] M. Jaihuni, J. K. Basak, F. Khan, F. G. Okyere, T. Sihalath, A. Bhujel, J. Park, D. H. Lee, and H. T. Kim, "A novel recurrent neural network approach in forecasting short term solar irradiance," *ISA Trans.*, vol. 121, pp. 63–74, Feb. 2022, doi: 10.1016/j.isatra.2021.03.043.

[183] A. M. Efendi, Y. Kim, and D. Choi, "LSTM-based multi-step SOC forecasting of battery energy storage in grid ancillary services," in *Proc. IEEE Int. Conf. Commun., Control, Comput. Technol. Smart Grids (SmartGridComm)*, Aachen, Germany, Oct. 2021, pp. 276–281, doi: 10.1109/SmartGridComm51999.2021.9632319.

[184] M. A. Mohandes, "Modeling global solar radiation using particle swarm optimization (PSO)," *Sol. Energy*, vol. 86, no. 11, pp. 3137–3145, Nov. 2012, doi: 10.1016/j.solener.2012.08.005.

[185] A. Hussain, Z. A. Khan, T. Hussain, F. U. M. Ullah, S. Rho, and S. W. Baik, "A hybrid deep learning-based network for photovoltaic power forecasting," *Complexity*, vol. 2022, pp. 1–12, Oct. 2022, doi: 10.1155/2022/7040601.

[186] H. Zang, L. Liu, L. Sun, L. Cheng, Z. Wei, and G. Sun, "Short-term global horizontal irradiance forecasting based on a hybrid CNN-LSTM model with spatiotemporal correlations," *Renew. Energy*, vol. 160, pp. 26–41, Nov. 2020, doi: 10.1016/j.renene.2020.05.150.

[187] D. So, J. Oh, I. Jeon, J. Moon, M. Lee, and S. Rho, "BiGTA-Net: A hybrid deep learning-based electrical energy forecasting model for building energy management systems," *Systems*, vol. 11, no. 9, p. 456, Sep. 2023, doi: 10.3390/systems11090456.

[188] G. Li, S. Xie, B. Wang, J. Xin, Y. Li, and S. Du, "Photovoltaic power forecasting with a hybrid deep learning approach," *IEEE Access*, vol. 8, pp. 175871–175880, 2020, doi: 10.1109/ACCESS.2020.3025860.

[189] G. Dra#us, D. Mazur, J. Kusznier, and J. Dra#us, "Application of artificial intelligence algorithms in multilayer perceptron and Elman networks to predict photovoltaic power plant generation," *Energies*, vol. 16, no. 18, p. 6697, Sep. 2023, doi: 10.3390/en16186697.

[190] R. Asghar, F. Riganti Fulginei, H. Wadood, and S. Saeed, "A review of load frequency control schemes deployed for wind-integrated power systems," *Sustainability*, vol. 15, no. 10, p. 8380, May 2023, doi: 10.3390/su15108380.

RAFIQ ASGHAR received the M.Sc. degree in electrical power engineering from the University of Engineering and Technology, Peshawar, in 2018. He is currently pursuing the Ph.D. degree in electrical engineering with Università degli Studi Roma Tre, Rome, Italy. His master's thesis focused on the design of an SMC-based MST-FCL to improve LVRT and provide reactive power for the DFIG wind turbine systems. His research interests include power system control, renewable energy integration, vehicle-to-grid (V2G) technologies, non-linear optimization, machine learning, and deep learning.

FRANCESCO RIGANTI FULGINEI is currently a Full Professor with Roma Tre University, Rome, Italy, where he teaches and directs research in non-linear optimization and inverse problems with the Department of Industrial, Electronics, and Mechanical Engineering. His research interests include artificial intelligence, non-linear optimization, and inverse problems applied to complex systems, particularly power electronics, electromagnetic devices, and renewable energy.

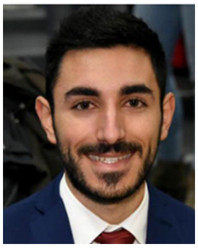

MICHELE QUERCIO was born in Avola, Sicily, Italy, in 1994. He received the bachelor's and master's degrees in mechanical engineering from the Politecnico di Torino, Turin, Italy, in 2016 and 2018, respectively, and the Ph.D. degree in electrical engineering from the Energy Department, in 2022. He works in several fields: computation of electromagnetic fields, design of magnetic shields, implementation of computational algorithms, renewable energy, and artificial intelligence. He is currently a Convenor of the working group on non-destructive testing applied to the additive manufacturing sector of Italian National Association of Non-Destructive Testing and a Vice-Convenor of the Same Commission WG6 (https://www.efndt.org/Organisation/WorkingGroups/Working-Group-6 NDT-in-Additive-Manufacturing) of European Federation for Non-Destructive Testing (EFNDT). He is also a Researcher with Università Degli Studi Roma Tre.

ASSIA MAHROUCH was born in Sefrou, Morocco, in 1992. She received the M.Sc. degree in renewable energies and storage from the Higher Normal School (École Normale Supérieure), Mohammed V University in Rabat, in 2016, and the Ph.D. degree from the Engineering for Smart and Sustainable Systems Research Center, Mohammadia School of Engineers, Mohammed V University in Rabat, in 2024. Her research interests include frequency regulation and voltage stability in microgrids, with a particular focus on artificial intelligence techniques, such as fuzzy logic controllers and artificial neural networks.

Open Access funding provided by 'Università degli Studi Roma Tre' within the CRUI CARE Agreement